Supplementary Information for

Formation of the intradimer disulfide bond in human calprotectin maintains metal-withholding function and tunes protein susceptibility

Aurelio Mollo,* Emma Y. Cool,* Bahar Sakar,* Kushol Gupta,† and Elizabeth M. Nolan*

*Department of Chemistry, Massachusetts Institute of Technology, Cambridge, MA 02139, United States

†Department of Biochemistry & Biophysics, Perelman School of Medicine, University of Pennsylvania, Philadelphia, PA 19104, United States

Corresponding author: Elizabeth M. Nolan (Email: lnolan@mit.edu, Tel: 617-452-2495)

This Supplementary Information includes:

Experimental Methods

Supplementary Discussion

Supplementary Figures

Supplementary Tables

Experimental Methods

General Materials and Methods

All solvents and chemicals were purchased from commercial suppliers and used as received. Buffers and metal solutions were prepared using Milli-Q water (18.2 MΩ•cm, 0.22-μm filter, Millipore). For pH adjustments, reagent-grade NaOH (EMSURE®, Sigma) and HCl (ACS grade, Sigma) were used. Unless otherwise specified, buffers were prepared using ultrahigh-purity grade HEPES (ULTROL® grade, Sigma), Tris (Ultra-Pure, VWR) and/or NaCl (Suprapur®, Sigma). To prevent metal contamination from glass, buffers were stored in polypropylene tubes and bottles.

In cases where even trace levels of metals could interfere with experiments, the buffers were mixed with Chelex® 100 resin (Bio-Rad, #142-2842, 10 g/L). Following an incubation period, the resin was removed by means of a 0.45-μm filter and the pH of the buffer readjusted.

Stock solutions of metal ions were prepared in acid-washed volumetric glassware, sterile-filtered, and stored in polypropylene containers. The concentrations and trace metal contamination levels of the various metal stocks were determined by inductively coupled plasma mass spectrometry (ICP-MS; see section below). For stock solutions of Fe(II), $(NH_4)_2Fe(SO_4)_2 \cdot 6H_2O$ powder was dissolved fresh in Milli-Q water immediately before the experiment. The sources of the metal stocks are reported in **Table S3**.

Protein concentrations were determined by A_{280} absorbance measurements. These were taken using a BioTek Synergy HT Microplate Reader, outfitted with a BioTek Take3 Microvolume Plate (0.048-cm pathlength). The concentration of CP was calculated using an extinction coefficient (ε) of 18,450 M^{-1} cm^{-1}, while the concentration of dslCP was calculated using an extinction coefficient of 18,575 M^{-1} cm^{-1}. The concentrations of other proteins were calculated using the extinction coefficients reported in **Table S4**.

Cell optical densities (ODs) were determined using a Beckman Coulter DU800 Spectrophotometer, using polypropylene cuvettes with a 1-cm pathlength and monitoring absorbance at 600 nm.

All experiments were performed in triplicate using at least two independent batches of protein. In the case of dsICP, a batch was defined as the product of an individual oxidation reaction, even when multiple oxidations were performed using the same starting CP preparation.

Expression and Purification of Calprotectin (CP) and Variants

CP, CP-Ser and CP-Ser^{I60E} were expressed, purified and handled according to previously established protocols.[S1,S2] The preparation of dsICP is detailed below.

General Microbiology

Luria broth (LB) and tryptic soy broth (TSB) were prepared according to vendor recommendations. Tris:TSB medium was prepared as a 62:38 v/v mixture of antimicrobial assay (AMA) buffer (20 mM Tris, 100 mM NaCl, pH 7.5) and TSB (with dextrose) and sterilized by passage through a 0.22-μm filter. Immediately prior to use, the medium was supplemented with 2 mM Ca(II). Chemically defined medium (CDM) was prepared as previously described,[S3] and supplemented with 1 mM Ca(II), 0.3 μM Mn(II), 0.1 μM Cu(II), 0.1 μM Ni(II), 5 μM Fe(II), and 6 μM Zn(II) before use. The bacterial strains listed in **Table S10** were streaked from freezer stocks onto LB agar plates and grown at 37 ºC overnight (16–20 h). Overnight liquid cultures were prepared by inoculating 2 mL of LB medium in 14-mL polypropylene culture tubes with five individual colonies. Overnight cultures were incubated at 37 ºC and 250 rpm for 12–16 h.

Western Blot Analysis of CP Subunits

To detect S100A8 and S100A9 subunits by Western blotting, protein samples (~20 μM) were mixed in equal parts with 2× SDS-PAGE loading dye and heated for 5–7 min at 95 ºC. For reduced control samples, the dye was supplemented with 2% v/v β-mercaptoethanol. 5–10 μL of

each sample was loaded onto a 15% polyacrylamide gel (5% stacking layer) and run at 150 V until the dye front fully cleared the gel. The gel was removed from the casting apparatus and submerged in 1× Turbo buffer (48 mM Tris, 39 mM glycine, 1 g/L SDS, pH 9.2, 20% EtOH). After a 5-min equilibration period, the gel was transferred to a nitrocellulose membrane using a semi-dry transfer sandwich and a Bio-Rad Trans-Blot Turbo™ machine (11 min, 15 V). The membrane was blocked for 1 h at room temperature with 10 mL of 5% milk in TBS (20 mM Tris pH 7.5, 138 mM NaCl) + 0.01% NaN_3. The membrane was quickly rinsed with 3 × 10 mL of Milli-Q water. Then, it was incubated overnight at 4 ºC with 10 mL of a 1:250 dilution of α-S100A8 mAb (AlexaFluor® 680 conjugate, Santa Cruz Biotechnology Inc., #sc-48352 AF680) and a 1:1,000 dilution of α-S100A9 mAb (AlexaFluor® 790 conjugate, Santa Cruz Biotechnology Inc., #sc-376772 AF790) in 5% BSA (TBS) + 0.01% NaN_3. In the morning, the membrane was brought to room temperature and was washed with 4 × 10 mL of TBS + 0.1% Tween-20 (10 min each). The membrane was rinsed twice with Milli-Q water and visualized using a LI-COR Odyssey DLX (700 nm and 800 nm channels).

Inductively Coupled Plasma Mass Spectrometry (ICP-MS)

The concentration of metal ions in either metal stock solutions or media was determined using an Agilent 7900 inductively coupled plasma mass spectrometer (ICP-MS). The instrument is located in the Center for Environmental Health Sciences Bioanalytical Core Facility at the Massachusetts Institute of Technology. The instrument was operated in Helium mode. Prior to each run, a series of standards were prepared using an environmental standard mixture containing 100 μg/mL of Ca, Fe, K, Mg and Na, and 10 μg/mL of Co, Cu, Mn, Ni and Zn (Agilent Technologies, #5183-4688). The mixture was diluted 1:10 → 1:100,000 in 10-fold serial dilutions, and standard curves plotted for each element. Included in the standards was a blank sample of 5% HNO3 (ARISTAR® ULTRA, Ultrapure for trace metal analysis, VWR, #87003-228). All blanks and all samples were prepared in 3–5% HNO_3 in Milli-Q water, and supplemented with an internal standard of 1 ppb Tb (Agilent Technologies, #5190-8590). Samples were prepared in 5-mL

polypropylene tubes (VWR, #470225-028) and transferred to 2-mL PTFE ICP-MS sample cups (PerkinElmer Life Sciences, #B3001566) for analysis.

Preparation of dslCP

dslCP was prepared by thawing 20–30 mg of CP on ice over 1 h. The solution was brought up to 10 mL with buffer (20 mM HEPES pH 8.0 + 1 mM NaCl) and injected into a pre-hydrated Slide-A-Lyzer® cassette (3–12 mL, 10-kDa MWCO; Fisher Scientific, #66810) or tubing (Spectra/Por3 RC Dialysis Membrane Tubing, 3.5-kDa MWCO). The cassette/tubing was placed in 5 L of room-temperature buffer, freshly supplemented with 20–35 μM H_2O_2 (Millipore Sigma, #18304). After 4 h of gentle stirring and again after 8 h, the cassette/tubing was transferred to a new 5 L buffer solution, also freshly supplemented with H_2O_2. After a total of 24 h, the contents of the cassette/tubing were diluted to 30 mL with 20 mM Tris pH 9.5 (no salt). To remove precipitates and any contaminating bacteria, the sample was filtered through a 0.22-μm cellulose acetate membrane (VWR, #76479-044). The sample was injected onto an anion exchange column (Capto™ HiRes Q 10/100, Cytiva, #29275881) connected to an ÄKTA FPLC system (UPC-10, Cytiva, #28406268). Following injection, the column was washed with 2 column volumes (CVs) of Buffer A (20 mM Tris pH 9.5 + 5 mM NaCl). Protein was eluted with a 10→30% gradient of Buffer B (20 mM Tris pH 9.5 + 1 M NaCl) over 15 CVs at 1 mL/min, with absorbance monitored at 280 nm. 20 μL of each fraction were mixed 1:1 with 2× SDS-PAGE loading dye (no reductant) and analyzed by SDS-PAGE. The fractions with the highest dslCP purity were combined and concentrated to ~2 mL using a 10-kDa MWCO spin concentrator (Millipore Sigma, #UFC801024). The solution was transferred to a pre-hydrated Slide-A-Lyzer® cassette (0.5–3 mL, 10-kDa MWCO; Fisher Scientific, #66380). The protein was dialyzed overnight in 1 L of storage buffer (20 mM HEPES pH 8.0 + 100 mM NaCl), supplemented with 10 g of Chelex®. In the morning, the sample was concentrated down to ~500 μL, aliquoted, and flash-frozen. The aliquots were stored at −80 ºC and thawed on ice prior to use. In some cases, aliquots were refrozen once, but never more than twice in total.

Protein concentration was determined using absorbance measurements as detailed under '*General Materials and Methods'*. A typical preparation involved one to three parallel oxidation reactions, which were combined prior to the anion exchange step and purified using a corresponding number of injections. Yields for a given preparation ranged from 15% to 40%, with purities commonly exceeding 90% as determined by SDS-PAGE analysis.

HPLC Analysis of CP Subunits and dslCP

Samples of CP and dslCP were prepared for and analyzed by HPLC using an established protocol.[S4] 36 μL of protein solution was mixed with 120 μL of 6 M Guanidine HCl and 4 μL of 6% v/v trifluoroacetic acid (TFA), then spun down at 13,000 rpm for 10 min. 120 μL of supernatant were transferred to an HPLC vial and analyzed using an Agilent 1260 Infinity HPLC, equipped with a C4 reverse-phase column (Proto 300 C4, 5 μm particle size, 300 Å pore size, 4.6×250 mm, Higgins Analytical Inc.) running at 1 mL/min. Gradient (A/B): 0.0 min, 10% B; 15.0 min, 40% B; 55.0 min, 45% B; 55.5 min, 100% B; 70.5 min, 100% B; 71.0 min, 10% B; 86.0 min, 10% B. Mobile phase A consisted of water + 0.1% (v/v) TFA, while mobile phase B consisted of acetonitrile + 0.1% (v/v) TFA. Acetonitrile and TFA were both purchased as HPLC-grade solvents (Sigma). The elution was monitored at 220 nm, with a 500 nm reference wavelength and 100 nm bandwidth. Under the specified gradient conditions, S100A8, S100A9, and dslCP eluted at approximately 33.0, 46.5, and 53.0 min, respectively. All integrations were performed using the instrument's built-in analysis software.

Quadrupole Time-of-Flight (Q-TOF) Detection of CP Subunits and dslCP

90 μL of a 200-μM solution of dslCP or CP was separated by reverse-phase HPLC using the method detailed above. Fractions corresponding to the main peaks were collected manually and lyophilized overnight. The dried fractions were each resuspended in 250 μL of 50:50 ACN/H_2O and pelleted at 13,000 rpm for 10 min. 175 μL of supernatant were transferred to an MS vial. 5 μL were injected onto an Agilent 6545 Q-TOF MS housed at the Massachusetts Institute

of Technology's Department of Chemistry Instrumentation Facility (DCIF), running in positive mode and equipped with an Agilent Poroshell StableBond C18 column (5 μm particle size, 300 Å pore size, 2.1×75 mm) running at 0.3 mL/min. Gradient (A/B): 0 min, 10% B; 1 min, 10% B; 7 min, 50% B; 14 min, 80% B; 16 min, 95% B; 17 min, 95% B; 18 min, 10% B. Mobile phase A consisted of water + 0.1% (v/v) formic acid (FA), while mobile phase B consisted of acetonitrile + 0.1% (v/v) FA. Acetonitrile and FA were both purchased as HPLC-grade solvents (Sigma). The mass spectra obtained were deconvoluted using the Agilent MassHunter BioConfirm software.

Tryptic MS Analysis of dslCP

An aliquot of dslCP was thawed on ice and buffer exchanged into trypsin reaction buffer (50 mM ammonium bicarbonate, pH 8.0). A total of six buffer-exchange cycles were performed, each consisting of a 5-fold dilution. The protein was then diluted with trypsin reaction buffer to a final volume of 500 μL and a final concentration of 30 μM, and trypsin was added to a final concentration of 1 μM. The reaction mixture was divided into two 250-μL aliquots, each of which was incubated overnight at 37 ºC and 200 rpm. After ~16 h, both reaction tubes were flash-frozen and lyophilized to remove ammonium bicarbonate.

One sample was resuspended in 200 μL of water + 0.1% FA and pelleted (13,000 × g, 10 min). 125 μL of supernatant was transferred to an MS vial. This sample corresponds to the no-TCEP condition.

The second sample was resuspended in 50 μL of water, and TCEP was added to a final concentration of 4 mM (2 μL of 0.1 M stock). The sample was incubated for 1 h at 37 ºC and 200 rpm, diluted to 200 μL with water, and supplemented with 0.1% TFA (0.8 μL of 25% stock). As above, the sample was pelleted by centrifugation (13,000 × g, 10 min) and 125 μL of supernatant was transferred to an MS vial. This sample corresponds to the +TCEP condition.

Both samples were analyzed by LC-QTOF MS using the protocol detailed in the preceding section. All data analysis was performed using the Agilent MassHunter Qualitative Analysis software.

Thiol Quantification Assay

The number of free cysteine residues in CP and dslCP was measured using a protocol adapted from previous work.[S5] In short, a 4 mM solution of 2,2'-dithiodipyridine (DTDP) was prepared by dissolving DTDP in 1 M HCl and then diluting with water to the desired DTDP concentration. The solution was aliquoted and stored at −20 ºC. On the day of the experiment, a 3 mM solution of reduced glutathione (GSH) was made fresh in 10 mM HCl. The assay buffer (100 mM NaH_2PO_4, 200 μM EDTA, pH 7.0) was degassed by bubbling N_2 through for >1 h prior to use.

Protein stocks were thawed on ice and buffer-exchanged into 20 mM NaOAc pH 5.0 using 10-kDa MWCO spin concentrators. A total of six buffer-exchange cycles were performed, each consisting of a 5-fold dilution. Protein solutions were kept on ice and used shortly thereafter.

A standard curve was generated by mixing 125 μL of DTDP stock with either 0, 10, 20, 30, or 40 μL of GSH stock and diluting to a final volume of 3 mL with assay buffer. The solutions were incubated at room temperature for 15 min, and the absorbance at 341 nm (A_{341}) was recorded; the DTDP-only sample served as the blank.

Alongside the control samples, protein samples were diluted to 12.5 μM with assay buffer to a final volume of 750 μL, including 31.25 μL of DTDP stock. Like the control samples, the solutions were incubated for 15 min at room temperature, and their A_{341} measured. The standard curve was used to determine the concentration of free thiols present in each protein sample.

Circular Dichroism (CD) Spectroscopy

Samples for CD spectroscopy were prepared by buffer exchanging dslCP or CP into 1 mM Tris pH 7.5 using 10-kDa MWCO spin concentrators. The buffer for CP also contained 1 mM DTT. CD spectra were obtained on a Jasco J-1500 CD spectrometer, located in the Biophysical Instrumentation Facility at the Massachusetts Institute of Technology. Spectra were recorded at room temperature with a protein concentration of 10 μM and using a CD cell from Hellma Analytics (1 mm pathlength). For samples containing Ca(II), 2 mM Ca(II) was added from a 50 mM stock

solution, and the solutions were incubated for at least 20 min prior to data collection. For thermal denaturation experiments, the same samples were heated with a ramp rate of 2 ºC/min from 25 ºC to 95 ºC.

Thermal denaturation curves were fitted to a Boltzmann sigmoidal function with sloped baselines using GraphPad Prism 10 (Equation 1), such that m_f and m_u are the slopes of the folded and unfolded regions of the curve, b_f and b_u are the absorbances of the folded and unfolded protein, m is the slope of the transition, T_m is the melting temperature, and T is the temperature (independent variable). Selected apo dslCP replicates were averaged and fitted to a two-transition curve (Equation 2). The subscript numbers attached to the variables signify the transition; u1 is the first transition and u2 is the fully unfolded protein.

(1) $$\frac{(m_f T+b_f)-(m_u T+b_u)}{1+e^{\frac{T-T_m}{m}}}+(m_u T+b_u)$$

(2) $$\frac{(m_f T+b_f)-(m_{u1} T+b_{u1})}{1+e^{\frac{T-T_{m_1}}{m_1}}}+\left(m_{u_1} T+b_{u_1}\right)+\frac{(m_{u2} T+b_{u2})*e^{\frac{T-T_{m2}}{m_2}}}{1+e^{\frac{T-T_{m_2}}{m_2}}}$$

Analytical Size Exclusion Chromatography (SEC)

Methods for analytical SEC were adapted from a previously reported protocol.[S1] Experiments were carried out on an ÄKTA FPLC system equipped with a Superdex™ 75 10/300 GL SEC column at 4 ºC. The column was equilibrated with running buffer (20 mM HEPES, 100 mM NaCl, pH 7.5) prior to each injection. The running buffer for the CP samples was supplemented with 5 mM DTT.

The column calibration was carried out by using a low molecular weight Gel Filtration Calibration Kit (Cytiva, #28403841). A 1-mg/mL solution of blue dextran was prepared for the dead volume determination. Following centrifugation for 10 min at 13,000 rpm and 4 ºC, the sample was injected onto the column. For the injection, 500 μL of sample solution was loaded onto a 100-μL loop and injected with 500 μL of running buffer. The sample was eluted over 1 CV

with a flow rate of 0.3 mL/min. Using the same method, a cocktail of protein standards was injected in a separate run. The cocktail contained 3 mg/mL of aprotinin (6.5 kDa), ribonuclease A (13.7 kDa), carbonic anhydrase (29 kDa), and conalbumin (75 kDa), and 4 mg/mL of ovalbumin (43 kDa). A standard curve was prepared for molecular weight calculations.

For experiments involving the absence or presence of Ca(II) in the running buffer, protein was diluted to 100 μM in buffer, which was supplemented with 0 mM or 2 mM Ca(II). Following a 15-min incubation in the respective buffer, the samples were injected onto the column. For the experiments involving a titration of varying Ca(II) concentrations, no Ca(II) was added to the running buffer. Instead, Ca(II) was added directly to the protein samples. The solutions, which contained 80 μM protein, were incubated for 25 min at room temperature prior to injection.

For the sample injections, 200 μL of sample solution was loaded onto a 100-μL loop and injected with 500 μL of running buffer. The sample was eluted over 1 CV with a flow rate of 0.3 mL/min.

Metal Depletion Assays

The workflow for metal depletion was adapted from a reported protocol.[S6] A 5-mL aliquot of bacterial growth medium was supplemented with either buffer (no-protein control) or 15 μM of dslCP, CP or CP-Ser. CDM was supplemented with 1 mM Ca(II), while Tris:TSB and Tris:YPD were supplemented with 2 mM Ca(II) to induce CP oligomerization. In the case of CP, 5 mM DTT was also added to the media to keep the protein reduced. The samples were incubated overnight at 30 ºC and 150 rpm. Meanwhile, a set of twelve centrifugal PES spin concentrators (10-kDa MWCO, Pall Corporation, #MAP010C38) were washed with 2 × 10 mL of 0.1 M EDTA pH 8.0 (1,000 × g, 10 min), followed by 10 × 10 mL rinses with Milli-Q water (3,000 × g, 6 min). After 24 h, the samples were transferred to the EDTA-washed filters and concentrated down to <1 mL (4,000 × g, 30 min). 3 × 4.03 mL of Milli-Q water were added to the retentate, which was spun down (4,000 × g, 30 min) after each addition. The combined flowthroughs (17.1 mL) were supplemented with 900 μL of HNO_3 and 1 ppb Tb and analyzed by ICP-MS. In addition to the

twelve samples prepared as above, a no-filter control was prepared by mixing 5 mL of fresh media with 12.1 mL of Milli-Q water and adding HNO_3 and 1 ppb Tb as above.

Antimicrobial (AMA) Assays

AMA assay protocols were adapted from previously reported procedures.[S7] Briefly, subcultures were prepared as 1:100 dilutions of the bacterial overnight cultures into 2 mL of LB medium in 14-mL polypropylene culture tubes. The subcultures were grown to an OD_{600} of ~0.6. The experimental media—Tris:TSB, Tris:YPD, and CDM—were inoculated with a 1:500 dilution of the subcultures. Each culture was treated with 10 μM dslCP, CP or CP-Ser that was buffer exchanged into AMA buffer using 10-kDa MWCO spin concentrators (Amicon). An equivalent volume of AMA buffer was added to the untreated controls, and the plates were sealed with a breathable seal (Breathe-Easy Sealing Membrane, Sigma). Bacterial growth was monitored over 18 h based on the absorbance at 600 nm in a 96-well plate using a BioTek LogPhase600 microbiology plate reader at 37 ºC and 700 rpm. Growth was monitored for 6 biological replicates, each with 2–3 technical replicates.

In the case of *C. albicans*, LB agar plates were streaked with the glycerol stock and incubated at 37 ºC overnight, then at room temperature for another 24 h to allow the colonies to reach a sufficient size for inoculation. Seed cultures were set up in the morning by transferring a single colony into 2 mL of YPD media using a sterile pipette tip, followed by shaking at 30 ºC, 300 rpm for ~4 h until the OD_{600} reached 0.6. The culture was then diluted 1:500 in Tris:YPD and used to set up AMA assays in the same manner as described above. The 96-well plates in the LP600 instrument were shaken at 37 ºC and 800 rpm, and monitored over the course of 22 h.

Chrome Azurol S (CAS) Assay

Protein for the CAS assays was prepared by buffer exchanging dslCP, CP or CP-Ser into AMA buffer three times using 10-kDa MWCO spin concentrators (Amicon). Overnight cultures were diluted 1:100 into 14-mL polypropylene culture tubes containing 1.4 mL of CDM and 15 μM

protein or AMA buffer (untreated control). The cultures were incubated at 37 ºC and 250 rpm for 8 h. The OD_{600} was measured, and the cultures were spun at 4,000 rpm and 4 ºC for 7 min. After the cells were spun down, the supernatants were stored in Eppendorf tubes at −20 ºC.

The universal CAS assay was carried out on bacterial supernatants according to the original protocol[S8] with the modifications made by Alexander et al.[S7,S9] The CAS dye solution was prepared immediately before use by dissolving 10.9 mg of hexadecyltrimethylammonium bromide (HDTMA, Spectrum Chemical) in ~12.5 mL of Milli-Q water with heating at 37 ºC. Separately, a $FeCl_3$ stock was prepared in an acid-washed volumetric flask by dissolving anhydrous $FeCl_3$ (trace metals basis) in water and HCl. The concentration of this stock solution was determined via ICP-MS, and the stock solution was subsequently diluted to 1 mM Fe, with a final HCl concentration of ~10 mM. A 750-μL aliquot of the 1 mM $FeCl_3$ stock solution was added to 3.75 mL of 2 mM Chrome Azurol S (MP Biomedicals). The mixture was slowly added to the HDTMA solution with stirring. Then, 25 mL of a 1 M MES buffer solution (pH 5.6, Millipore Sigma) was added slowly with stirring. The solution was transferred to an acid-washed volumetric flask and diluted with Milli-Q water to 50 mL. 5-sulfosalicylic acid (MP Biomedicals) was added as a solid to a final concentration of 4 mM, and the solution was filtered with a 0.22-μm filter. All solutions were kept at or above room temperature to avoid precipitation.

Prior to the assay, the supernatants were thawed, spun down at 13,000 rpm and 4 ºC for 10 min, and warmed to room temperature. The CAS assay was conducted in a 96-well plate. Each well was filled with 10 μL of supernatant, 90 μL of 0.5 M MES buffer to dilute the supernatant, and 100 μL of CAS dye solution (for *S. aureus* supernatants, 20 μL of supernatant and 80 μL of buffer were used instead). The plates were incubated in the dark at 30 ºC for 45 min. The absorbance at 630 nm was measured with a BioTek Synergy HT Microplate Reader. The siderophore content was determined with Equation 3:

(3) $$(A_{reference} - A_{sample})/A_{reference}$$

… where $A_{reference}$ is the A_{630} of replete CDM and A_{sample} is the A_{630} of the sample. The values were normalized to the cell content by multiplying each value by 10 to account for the supernatant dilution (or 5 for *S. aureus*) and dividing the calculated value by the OD_{600} of the cultures.

E. coli CFT073 demonstrated variable growth across biological replicates upon treatment with 15 μM dslCP, CP or CP-Ser. Hence, only the biological replicates with considerable growth, or an OD_{600} > 1, across all treatment conditions were used for analysis. Moreover, supernatants from this strain demonstrated minor precipitation (as determined by a higher A_{850} value than other samples), but its influence on the absorbance was negligible relative to the differences in A_{630} values between treated and untreated cultures.

Protease Susceptibility Assays

Protease susceptibility assays were adapted from a previous protocol.[S10] To monitor susceptibility to HNE, stock solutions of dslCP, CP-Ser and CP-Ser^{I60E} were diluted to 30 μM in 1× buffer (75 mM HEPES pH 7.5, 100 mM NaCl, 3 mM $CaCl_2$) and incubated for 1 h at 37 ºC, 175 rpm to allow for self-association. Samples were supplemented with 30 μM $MnCl_2$ (1 equiv) as needed. After the incubation period, 36 μL of the mixture were prepared for HPLC. The remaining volume was split into 36-μL aliquots, supplemented with 2.5 μM human neutrophil elastase (HNE; Fisher Scientific, #IHUELASD100UG), and incubated at 37 ºC, 175 rpm. After 15 min, 30 min, 1 h, 2 h, 4 h and 6 h, one aliquot was removed from the incubator. Samples were prepared for and analyzed by HPLC as detailed under '*HPLC Analysis of CP Subunits and dslCP*'.

Reactions with trypsin were performed the same way, except that the protein was treated with 1 μM trypsin (Affymetrix, #22725).

SV-AUC Analysis of dslCP and CP-Ser

SV-AUC analysis was carried out using a reported protocol with modifications.[S10] Protein samples (27.5 μM) were prepared in metal-free 75 mM HEPES pH 7.5, 100 mM NaCl and supplemented with either: (1) 1.35 mM EDTA ("apo"); (2) 20 equiv Ca(II) (550 μM); (3) 2 mM

Ca(II) (physiological concentration); or (4) 20 equiv Ca(II) (550 μM) + 1 equiv Mn(II) (27.5 μM). After a 30-min wait to allow for oligomerization, the samples were flash-frozen with liquid nitrogen and stored at −80 ºC until the day of the analysis.

Sedimentation velocity analytical ultracentrifugation (SV-AUC) experiments were performed at 20 ºC using an Optima analytical ultracentrifuge (Beckman Coulter, Brea, CA) equipped with a TiAn50 rotor. The instrument is housed at the Johnson Foundation Biophysical and Structural Biology Core Facility (University of Pennsylvania, Philadelphia PA). Samples were loaded into two-channel, charcoal-filled Epon centerpieces with sapphire windows, and data were collected using both absorbance and interference optics. Samples were thawed on wet ice and loaded into leak-tested SV-AUC cells. Loaded cells were allowed to equilibrate in the instrument under a temperature of 20 ºC and full vacuum for 1 h before experiments were initiated. Sedimentation velocity centrifugation was performed at 40,000 rpm and 20 ºC. Refractive index and absorbance data (260, 280 nm) were collected simultaneously every 30 seconds to record the radial concentration as a function of time until all the sedimenting components cleared the optical path (~6 h).

Data were fitted using the *c(S)* and *c(S,f/f$_0$)* implementations of the Lamm equation as implemented in the program SEDFIT version 17. The partial specific volume ($\bar{\upsilon}$), solvent density (ρ), and viscosity (η) were derived from chemical composition by SEDNTERP. Sedimentation coefficients were corrected for $S_{20,w}$.

Midpoint Potential (E_m) Determination of dslCP

The midpoint potential of dslCP was determined using a protocol adapted from previously reported methods.[S11,S12] Protein was thawed on ice over 1 h, purged with Argon gas, and transferred to a wet anaerobic chamber (Vacuum Atmospheres Co., Hawthorne CA). Separately, DTT_{red} and DTT_{ox} powders were also transferred to the chamber and resuspended in degassed Milli-Q water to form 1 mM and 150 mM stocks, respectively. Protein was diluted to 20 μM using buffer (75 mM HEPES, 100 mM NaCl, pH 7.00 ± 3 mM $CaCl_2$), and supplemented with

DTT_{red}/DTT_{ox}. The concentrations of the two redox components varied based on the desired voltage, with their sum fixed at 100 mM (see Supplementary Discussion). The reaction tubes (20 μL) were placed inside a sealed glass chamber saturated with water, and incubated for 24 h at 37 ºC inside the glovebox. After the incubation period, 5 μL of 310 mg/mL N-ethylmaleimide in DMSO were added to each tube, followed by vortexing and a 10-min incubation period. The samples were removed from the glovebox and mixed with 25 μL of 2× SDS-PAGE loading dye, then heated for 5–7 min at 95 ºC. 5 μL of each sample were run on a polyacrylamide gel (5% stacking, 15% resolving) and stained with Coomassie dye. The destained gels were visualized using an AlphaImager HP system (Cell Biosciences).

Thioredoxin Susceptibility Assays

The protocol to assess the thioredoxin susceptibility of dslCP was adapted from a prior report.[S11] In short, a 20-μM solution of dslCP was incubated in reaction buffer (75 mM HEPES, 100 mM NaCl, pH 7.00) in the presence of ± 2 mM $CaCl_2$ and ± 1 equiv $MnCl_2$ / 1.9 equiv $ZnSO_4$. 1.9 equiv of Zn(II) were used instead of the stoichiometric 2 equiv to avoid having free Zn(II) in solution due to any error in concentration or pipetting, which could potentially poison the selenocysteine-containing active site of TrxR.[S13–S15] After 1 h at room temperature, 20 μL of sample were set aside as the 0 h timepoint. Then, the reaction mix was supplemented with 2.5 μM human thioredoxin (Sigma Aldrich, #T8690), 0.05 μM rat liver thioredoxin reductase (Sigma Aldrich, #T9698) and 2.5 mM NADPH (Sigma Aldrich, #481973). The reaction was quickly split into 20-μL aliquots. The aliquots were kept at room temperature and quenched after the appropriate times. Samples were quenched via addition of 2.22 μL of 100 mM N-ethylmaleimide in DMSO (made fresh from powder on the day of use), followed by vortexing and incubation at room temperature for 10 min.

For HPLC analysis, samples were diluted to 36 μL with water, followed by a similar treatment and analysis workflow to the HNE samples. In the case where the sample was reduced prior to HPLC analysis, the 36-μL sample was mixed with 120 μL of 20 mM Tris pH 7.0 + 6 M

Guanidine HCl + 50 mM TCEP and heated at 95 ºC for 10 min. Upon cooling to room temperature, the TFA was added.

For the purposes of Western blot analysis, samples were mixed with 22.22 μL of 2× SDS-PAGE loading dye (no reductant), and analyzed as described in a prior methods section.

Supplementary Discussion

Determining the Midpoint Potential by Fitting to Nernst-Type Models

The midpoint potential (E_m) of a disulfide bond describes the voltage at which the concentrations of oxidized and reduced forms are equal ([red] = [ox]). The voltage established by a redox pair is described by the Nernst equation:

$$E = E^{\circ'} - \frac{RT}{nF} \ln \frac{[\mathrm{Red}]}{[\mathrm{Ox}]} \tag{4}$$

For a DTT_{ox}/DTT_{red} redox pair at pH 7.00 and 37 ºC: Eº' = −0.330 V,[1] R = 8.314 J K^{-1} mol^{-1}, T = 310.15 K and F = 96485 C mol^{-1} e^{-1}. This results in the following Nernst equation describing the concentrations of reduced and oxidized species:

$$E = -0.330 - \frac{0.0267267}{n} \ln \frac{[\mathrm{Red}]}{[\mathrm{Ox}]} \tag{5}$$

Now, for a DTT_{ox}/DTT_{red} redox pair, n = 2. This leads to the following equation:

$$E = -0.330 - 0.013363 \ln \frac{[\mathrm{Red}]}{[\mathrm{Ox}]} \tag{6}$$

If we let the independent variable X be the solution potential (mV) computed from the DTT_{ox}/DTT_{red} ratio and the dependent variable Y describe the % of oxidized species, we can rearrange Equation 6 to:

$$Y = \frac{100}{1 + \exp\left(-\frac{2}{26.7267}\left(X - E_m\right)\right)} = \frac{100}{1 + \exp\left(-\frac{X - E_m}{13.363}\right)} \tag{7}$$

A single-parameter fit (variable E_m) of the experimental % $HD5_{ox}$ data is shown in Figure **S38A–B**. Clearly, the fit displays a slope that is too shallow. This is because, in reality, n might differ from 2 owing to competing factors such as steric considerations, parallel microstates, or kinetic trapping.

In response, we can keep n as a variable, and if we let Y = % $HD5_{ox}$ and X = solution mV as before, we can rearrange Equation 5 to:

[1] This is usually reported for the standard state of 25 ºC. The temperature dependence of Eº' is small, so assuming the 25 ºC value at 37 ºC is a reasonable approximation.

$$Y = \frac{100}{1 + \exp\left(-\frac{n}{26.7267}(X - E_m)\right)} \tag{8}$$

A two-parameter fit (variables n and E_m) of the experimental % $HD5_{ox}$ data is shown in **Figure S38C–D**. The fit is much improved, but still relies on the assumption that the system reaches equilibrium at both high and low redox potentials relative to the E_m. In reality, our system only reaches ~80% $HD5_{ox}$ at high mV values relative to the E_m. To address this, the Nernst equation (5) can be rewritten as:

$$Y = Y_{\min} + \frac{Y_{\max} - Y_{\min}}{1 + \exp\left(-\frac{2h}{26.7267}(X - E_m)\right)} \tag{9}$$

… where n is replaced by the assumption of a $2e^-$ reaction with a "Hill-like" steepness factor, h, and Y_{min} and Y_{max} are now stated explicitly. Using this equation, we can fit h, E_m, Y_{min} and Y_{max}, as was done in prior work on S100A7 E_m determination.[S11] The results of the fit are shown in **Figure 8B** of the main text and are much more representative of the dataset. **Tables S14–S15** report the results of the various fits.

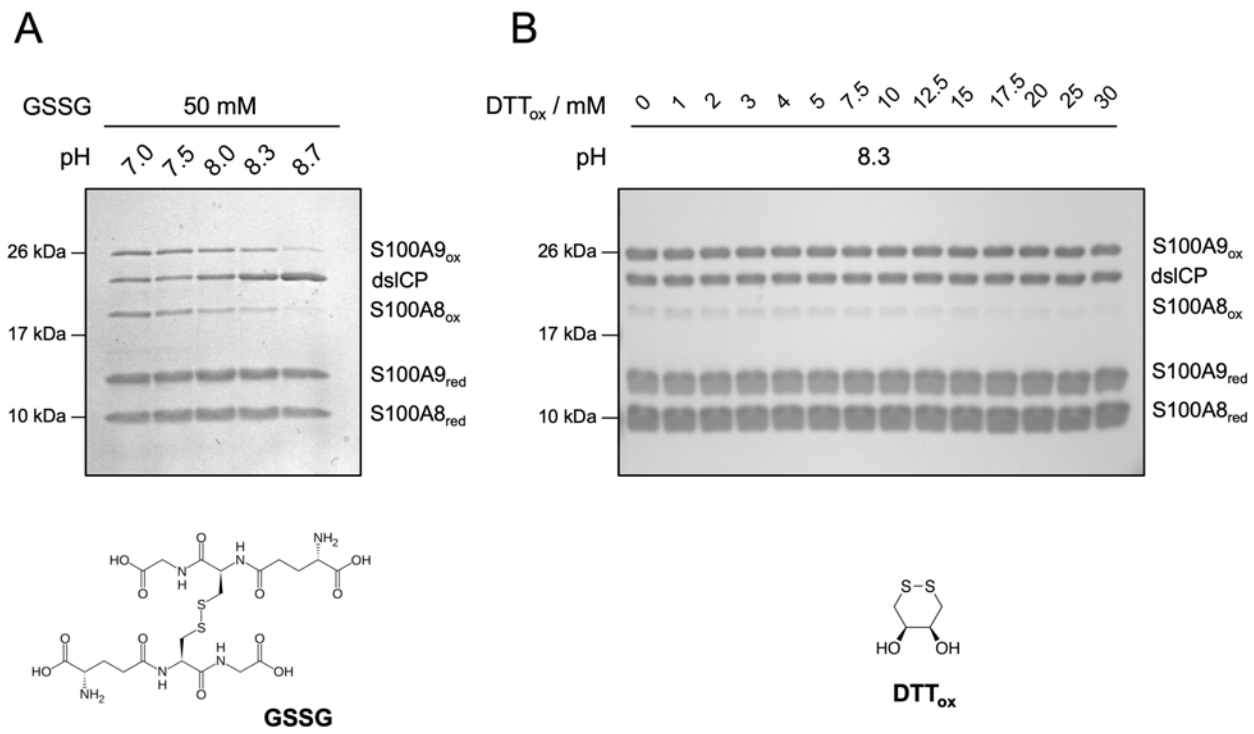

Figure S1. Prolonged incubation of CP with (A) GSSG or (B) DTT_{ox} results in little or no formation of disulfide-linked CP (dslCP), respectively. (A) CP (1 mg/mL) was incubated with GSSG (50 mM) for 72 h at room temperature at the indicated pH values in buffer containing 100 mM Tris and 200 mM NaCl (pH 7.0–8.7). (B) CP (1 mg/mL) was incubated with DTT_{ox} (0–30 mM) for 24 h at room temperature in buffer containing 100 mM Tris and 200 mM NaCl (pH 8.3). The chemical structure of each oxidizing compound is shown below its corresponding panel.

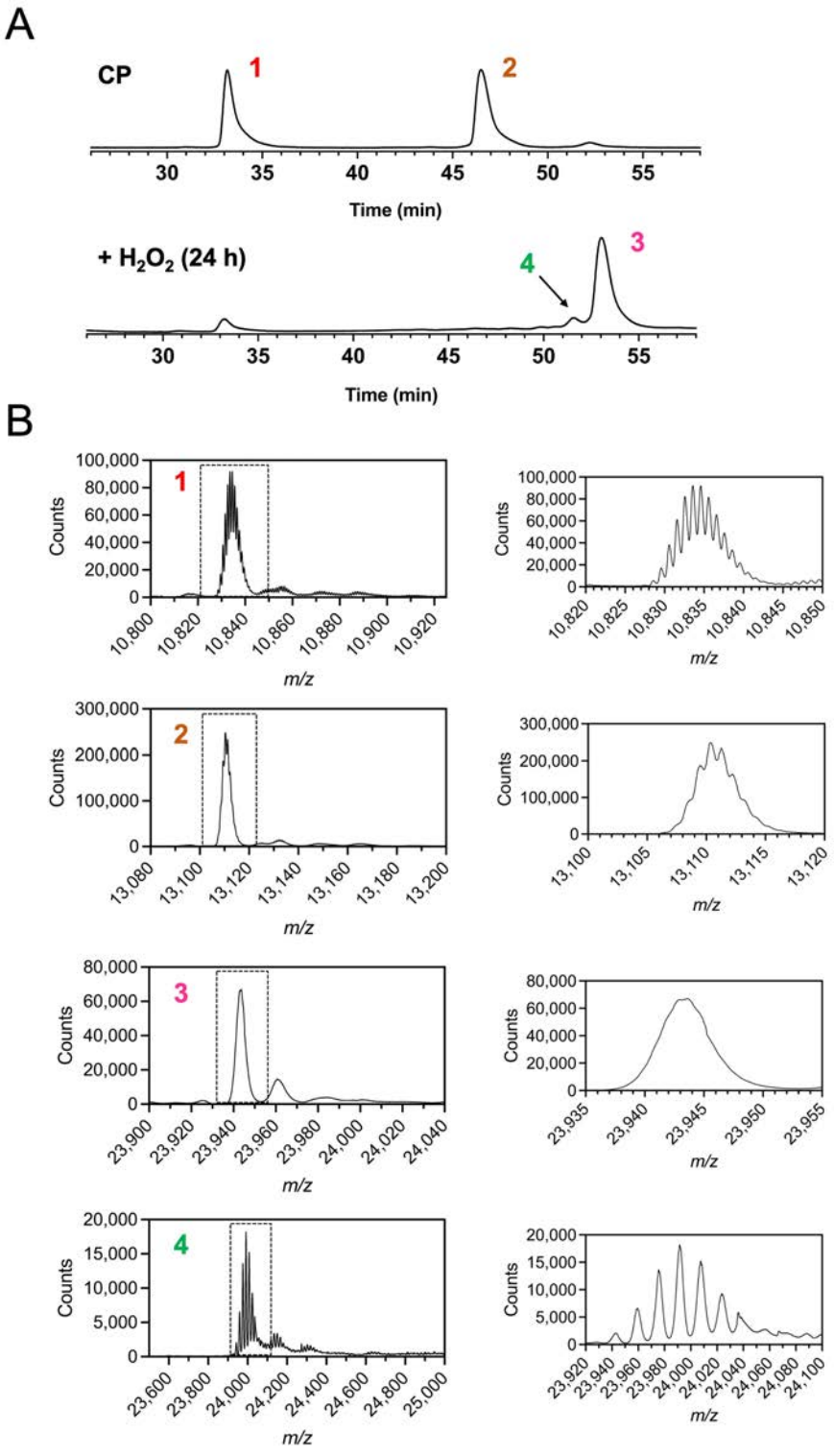

Figure S2. Q-TOF-MS detection of CP, dslCP and dslCP-MetO. (A) HPLC chromatograms of CP starting material, and CP + 100 μM H_2O_2 after 24 h. Peaks are labeled #1–4. (B) LC-Q-TOF-MS spectra of peaks labeled in A, with zoomed-in sections shown right. Peak 4 corresponds to dslCP-MetO, eluting earlier than dslCP and containing 1–6 oxidized methionines. See **Table S5**.

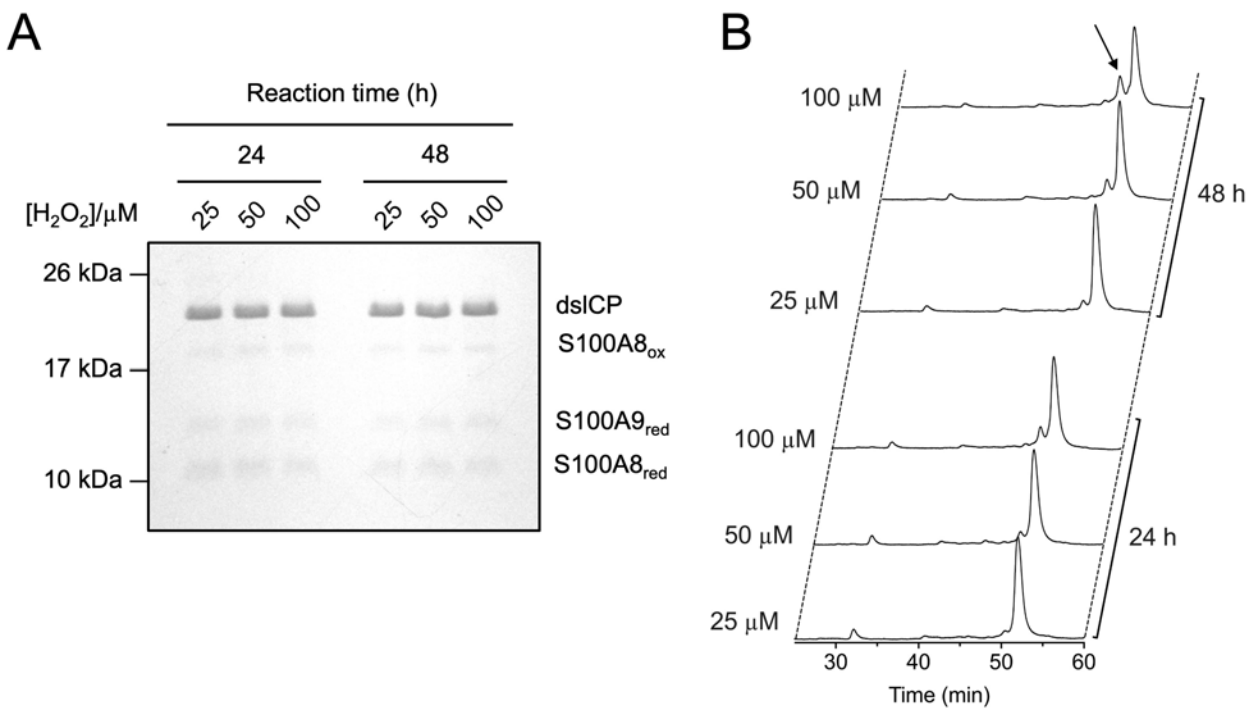

Figure S3. Optimized oxidation conditions for dslCP formation showing that 25 μM H_2O_2 leads to minimal methionine oxidation. (A) SDS-PAGE gel of 24- and 48-h reaction timepoints of CP in the presence of 25, 50 and 100 μM H_2O_2. The dslCP band intensity and migration pattern appear unchanged across H_2O_2 concentrations, thereby masking underlying differences in methionine oxidation. (B) HPLC chromatograms of the reactions from part A. A clear dslCP-MetO shoulder peak becomes visible with $[H_2O_2]$ > 25 μM and longer reaction times (see arrow).

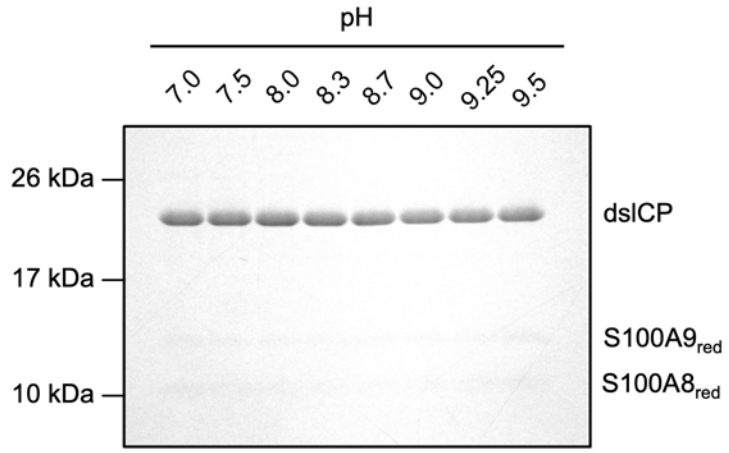

Figure S4. Oxidation of CP to dslCP is not pH-dependent between pH 7.0 and 9.5. CP (40 μM) was incubated with 100 μM H_2O_2 in 100 mM Tris buffer (pH 7.0–9.5) containing 200 mM NaCl. After 48 h, samples were analyzed by SDS-PAGE, revealing comparable formation of dslCP across all conditions.

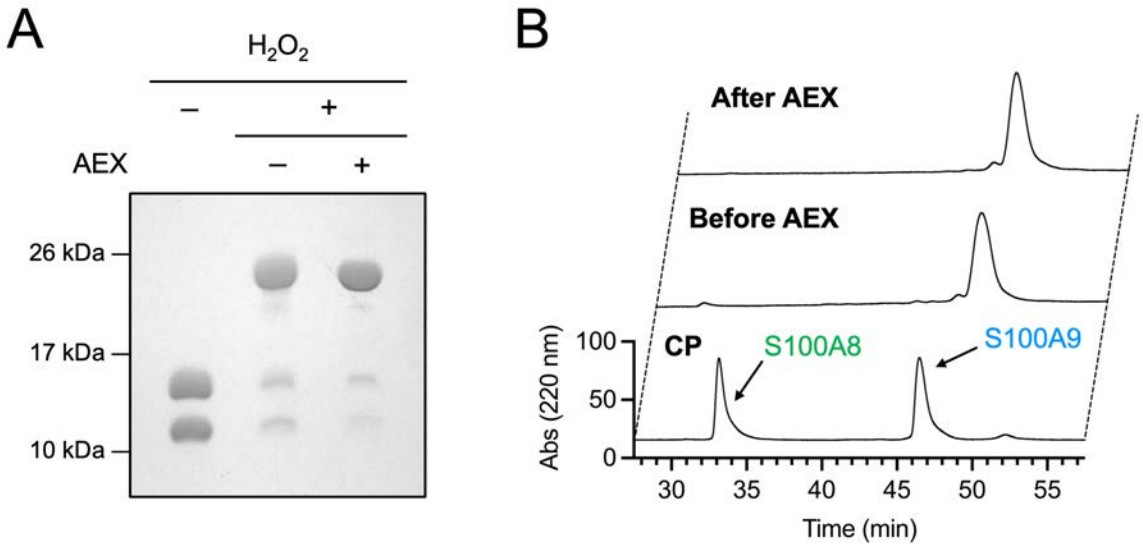

Figure S5. Anion exchange chromatography of the dslCP preparation. (A) SDS-PAGE analysis of CP starting material along with H_2O_2 reaction mixture prior to and following anion exchange chromatography (AEX). CP was incubated in the presence of 25 μM H_2O_2 for 24 h in 20 mM HEPES pH 8.0, 1 mM NaCl. (B) Associated HPLC chromatograms. S100A8 and S100A9 peaks are indicated.

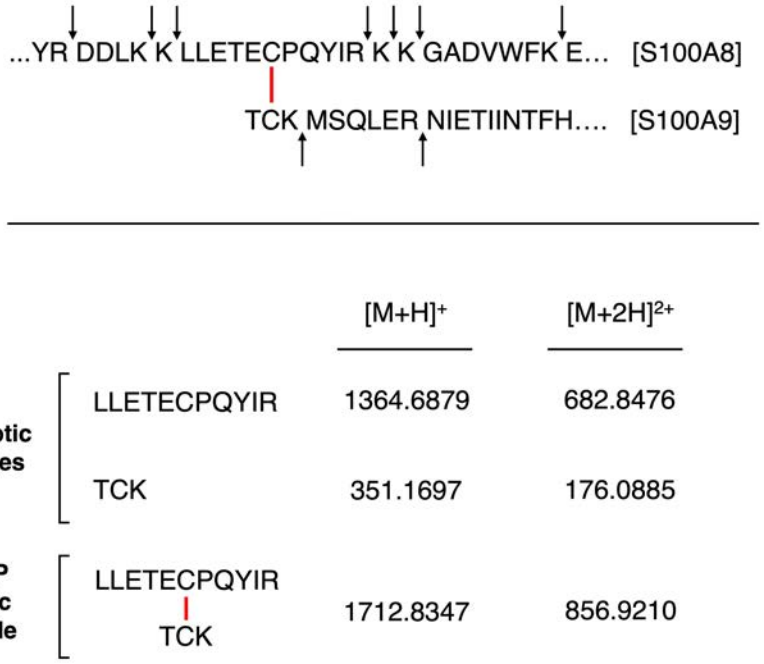

		[M+H]$^{+}$	[M+2H]$^{2+}$
CP tryptic peptides	LLETECPQYIR	1364.6879	682.8476
	TCK	351.1697	176.0885
dslCP tryptic peptide	LLETECPQYIR | TCK	1712.8347	856.9210

Figure S6. Partial amino acid sequences of S100A8 and S100A9 (*top*) and their associated tryptic peptides of interest (*bottom*). Expected *m/z* values for the +1 and +2 protonated ions are indicated. The location of the disulfide bond in dslCP is denoted in red. Locations of trypsin cut sites are indicated by black arrows. See **Table S7** for calculated and theoretical *m/z* values.

A

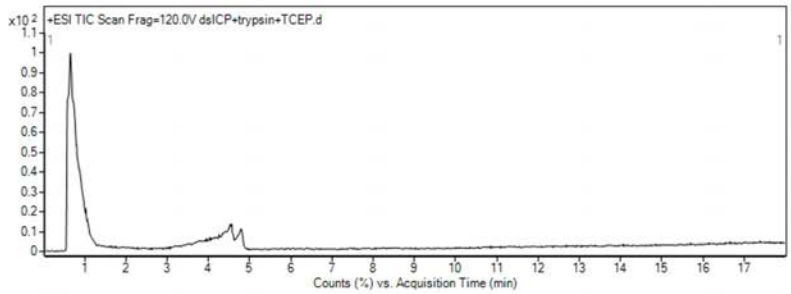
+ESI TIC Scan Frag=120.0V dsICP+trypsin+TCEP.d
Counts (%) vs. Acquisition Time (min)

B

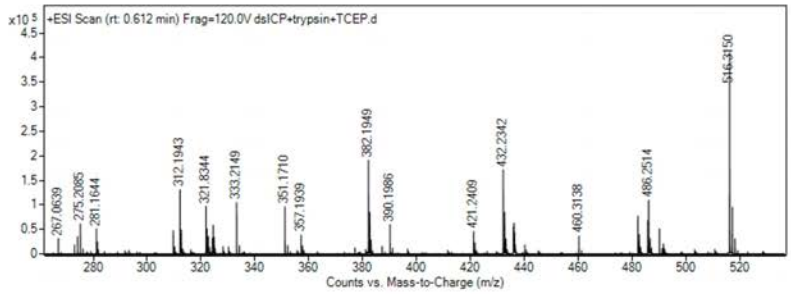
+ESI Scan (rt: 0.612 min) Frag=120.0V dsICP+trypsin+TCEP.d
267.0639
275.2085
281.1644
312.1943
321.8344
333.2149
351.1710
357.1939
382.1949
390.1986
421.2409
432.2342
460.3138
486.2514
516.3150
Counts vs. Mass-to-Charge (m/z)

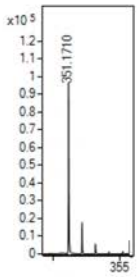
351.1710

C

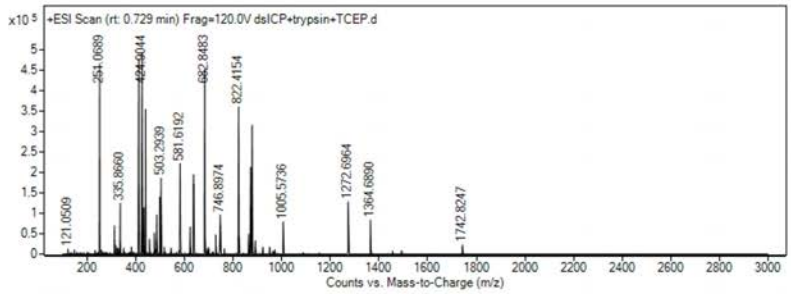
+ESI Scan (rt: 0.729 min) Frag=120.0V dsICP+trypsin+TCEP.d
121.0509
254.0689
335.8660
424.9044
503.2939
581.6192
682.8483
746.8974
822.4154
1005.5736
1272.6964
1364.6890
1742.8247
Counts vs. Mass-to-Charge (m/z)

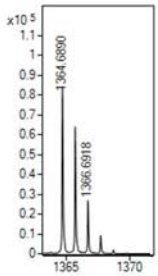
1364.6890
1366.6918

D

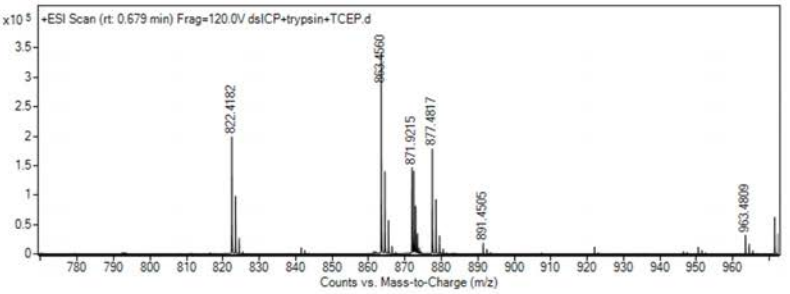
+ESI Scan (rt: 0.679 min) Frag=120.0V dsICP+trypsin+TCEP.d
822.4182
863.4560
871.9215
877.4817
891.4505
963.4809
Counts vs. Mass-to-Charge (m/z)

E

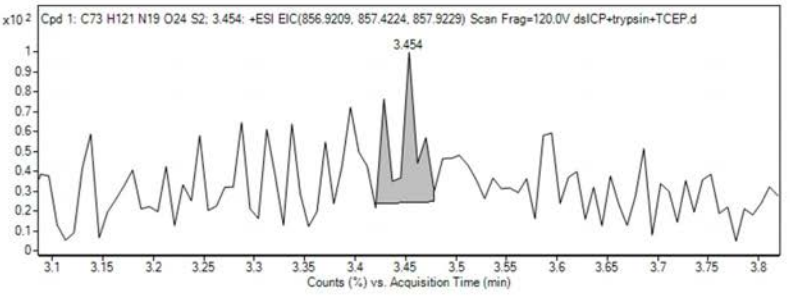
Cpd 1: C73 H121 N19 O24 S2; 3.454: +ESI EIC(856.9209, 857.4224, 857.9229) Scan Frag=120.0V dsICP+trypsin+TCEP.d
3.454
Counts (%) vs. Acquisition Time (min)

Figure S7. Analysis of TCEP-treated dslCP tryptic digestion products. (A) Total ion chromatogram (TIC) of the TCEP-treated tryptic digest. (B) MS spectrum at 0.612 min, showing the presence of multiple species including an ion at *m/z* 351.1710, corresponding to the TCK peptide. A close-up of this ion and its isotopic pattern is shown on the right. (C) MS spectrum at 0.729 min, showing the presence of multiple species including an ion at *m/z* 1364.6890, corresponding to the LLETECPQYIR peptide. A close-up of this ion and its isotopic pattern is shown on the right. (D) MS spectrum at 0.679 min, the retention time at which the disulfide-linked LLETECPQYIR–TCK tryptic product elutes in the non-reduced sample and is detected as the 2+ ion (**Figure S8**). No peak around *m/z* ~856.92 is visible here. (E) Supporting the observation in panel D, the extracted ion chromatogram shows no detectable presence of a species with the disulfide-linked peptide's molecular formula. Theoretical and observed *m/z* values for the tryptic peptides analyzed in panels B–E are reported in **Table S7**.

A

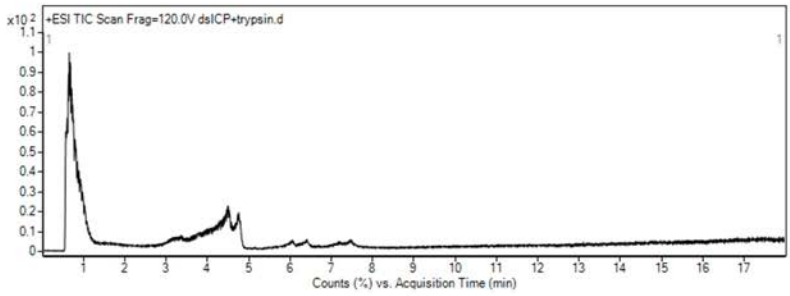
+ESI TIC Scan Frag=120.0V dsICP+trypsin.d
Counts (%) vs. Acquisition Time (min)

B

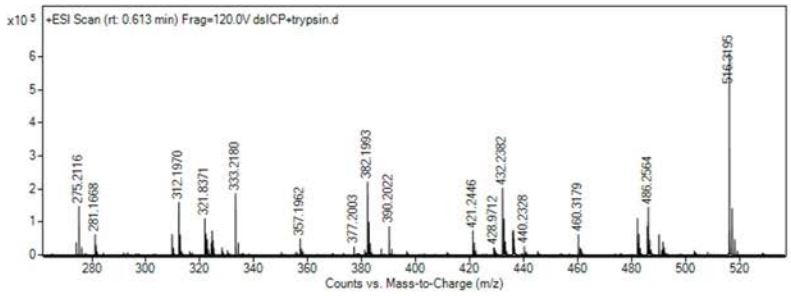
+ESI Scan (rt: 0.613 min) Frag=120.0V dsICP+trypsin.d
275.2116
281.1668
312.1970
321.8371
333.2180
357.1962
377.2003
382.1993
390.2022
421.2446
428.9712
432.2382
440.2328
460.3179
486.2564
516.3195
Counts vs. Mass-to-Charge (m/z)

C

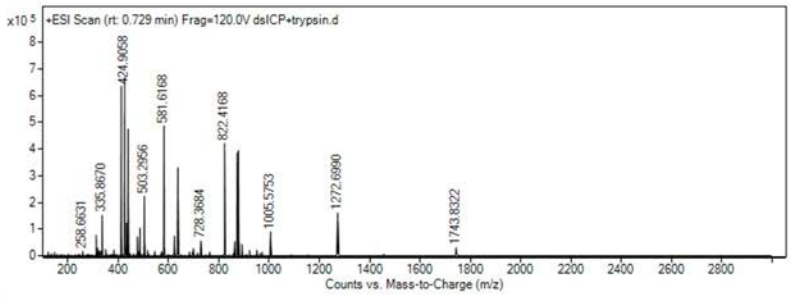
+ESI Scan (rt: 0.729 min) Frag=120.0V dsICP+trypsin.d
258.6631
335.8670
424.9068
503.2956
581.6168
728.3684
822.4168
1005.5753
1272.6990
1743.8322
Counts vs. Mass-to-Charge (m/z)

D

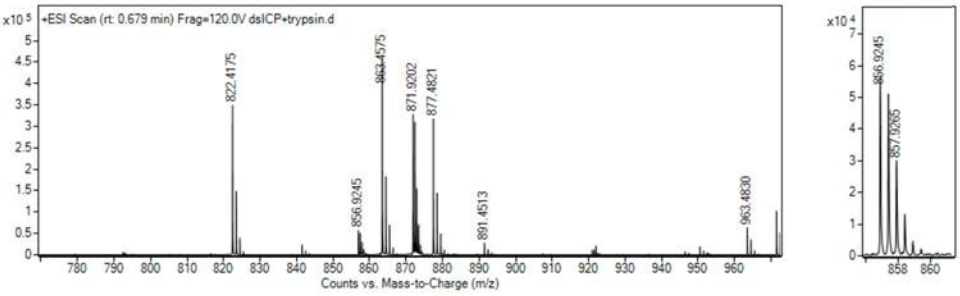
+ESI Scan (rt: 0.679 min) Frag=120.0V dsICP+trypsin.d
822.4175
856.9245
863.4575
871.9202
877.4821
891.4513
963.4830
Counts vs. Mass-to-Charge (m/z)
856.9245
857.9265

E

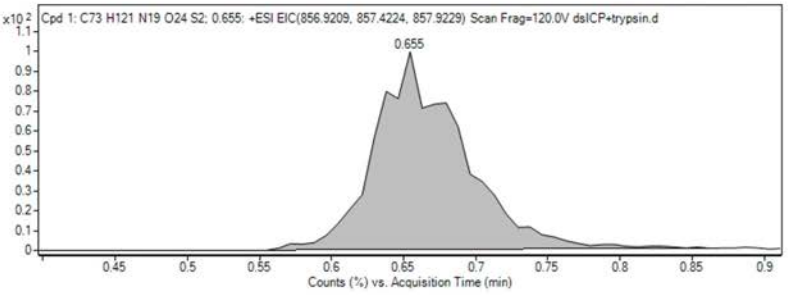
Cpd 1: C73 H121 N19 O24 S2: 0.655: +ESI EIC(856.9209, 857.4224, 857.9229) Scan Frag=120.0V dsICP+trypsin.d
0.655
Counts (%) vs. Acquisition Time (min)

Figure S8. Analysis of dslCP tryptic digestion products (no reductant added). (A) Total ion chromatogram (TIC) of the tryptic digest. (B) MS spectrum at 0.612 min, the retention time at which the TCK tryptic product elutes in the reduced sample (**Figure S7**). No peak at *m/z* ~351.17 is visible here. (C) MS spectrum at 0.729 min, the retention time at which the LLETECPQYIR tryptic product elutes in the reduced sample (**Figure S7**). No peak at *m/z* ~1364.69 is visible here. (D) MS spectrum at 0.679 min, showing the presence of multiple species including an ion at *m/z* 856.9245, corresponding to the disulfide-linked LLETECPQYIR–TCK tryptic product, detected as the 2+ ion. A close-up of this ion and its isotopic pattern is shown on the right. (E) The extracted ion chromatogram (EIC) for the *m/z* 856.9210 (2+) species demonstrates the presence of the disulfide-linked LLETECPQYIR–TCK product observed in panel D, with a peak elution time around 0.655 min post-injection. Theoretical and observed *m/z* values for the tryptic peptides analyzed in panels B–E are reported in **Table S7**.

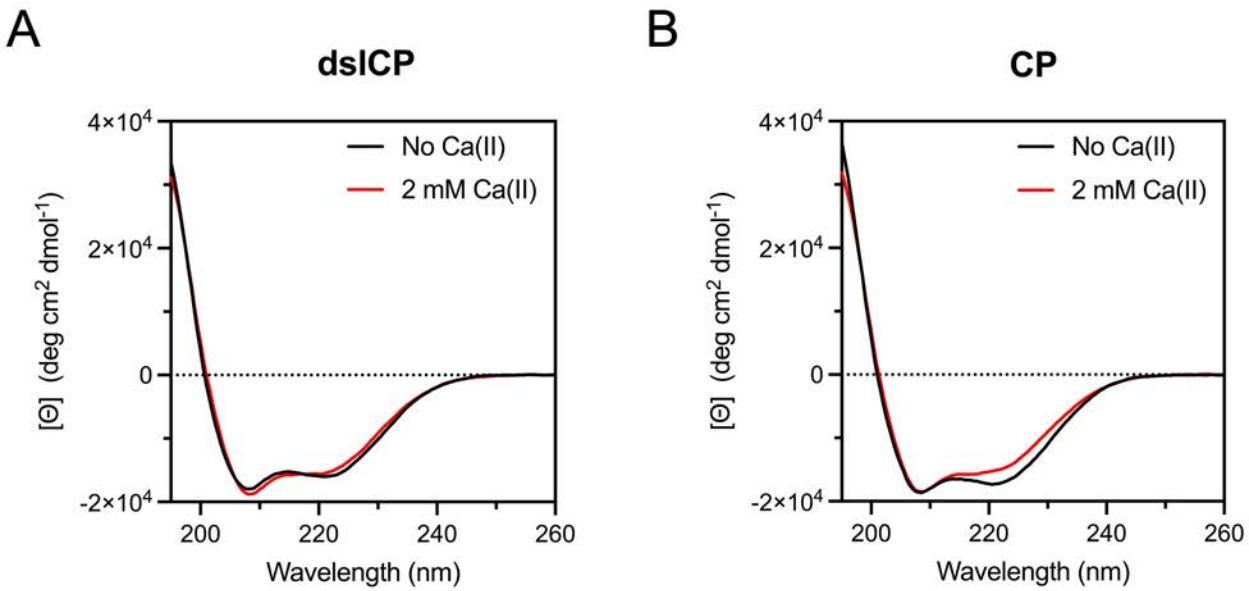

Figure S9. dslCP and CP exhibit similar α-helical content in the absence and presence of Ca(II). CD spectra of 10 μM (A) dslCP and (B) CP in the absence and presence of 2 mM Ca(II) are shown.

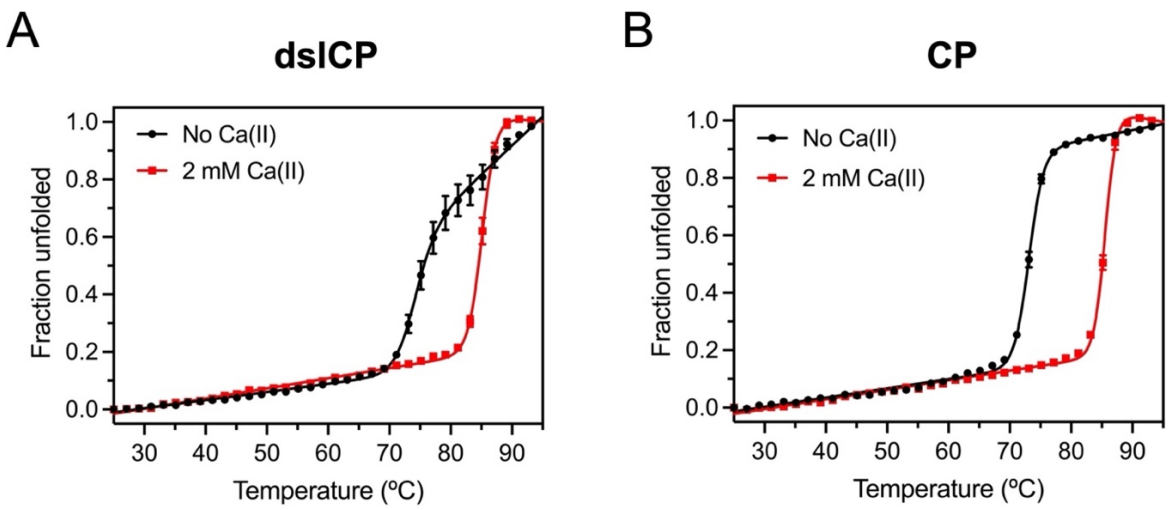

Figure S10. dslCP and CP display increased thermal stabilities in the presence of 2 mM Ca(II). Thermal denaturation curves for (A) dslCP and (B) CP were recorded by monitoring the absorption at 222 nm for 10 μM protein in 1 mM Tris pH 7.5 buffer with a 2-ºC/min ramp rate. Values are reported as mean ± s.e.m.; *n* = 3, except for dslCP −Ca(II), for which *n* = 10. The data points were fitted to a single-transition Boltzmann sigmoidal model (see Equation 1 in the Methods section), shown as a solid line. The averaged data for apo dslCP in panel A correspond to the averaged data from the 10 replicates shown in **Figure S11**.

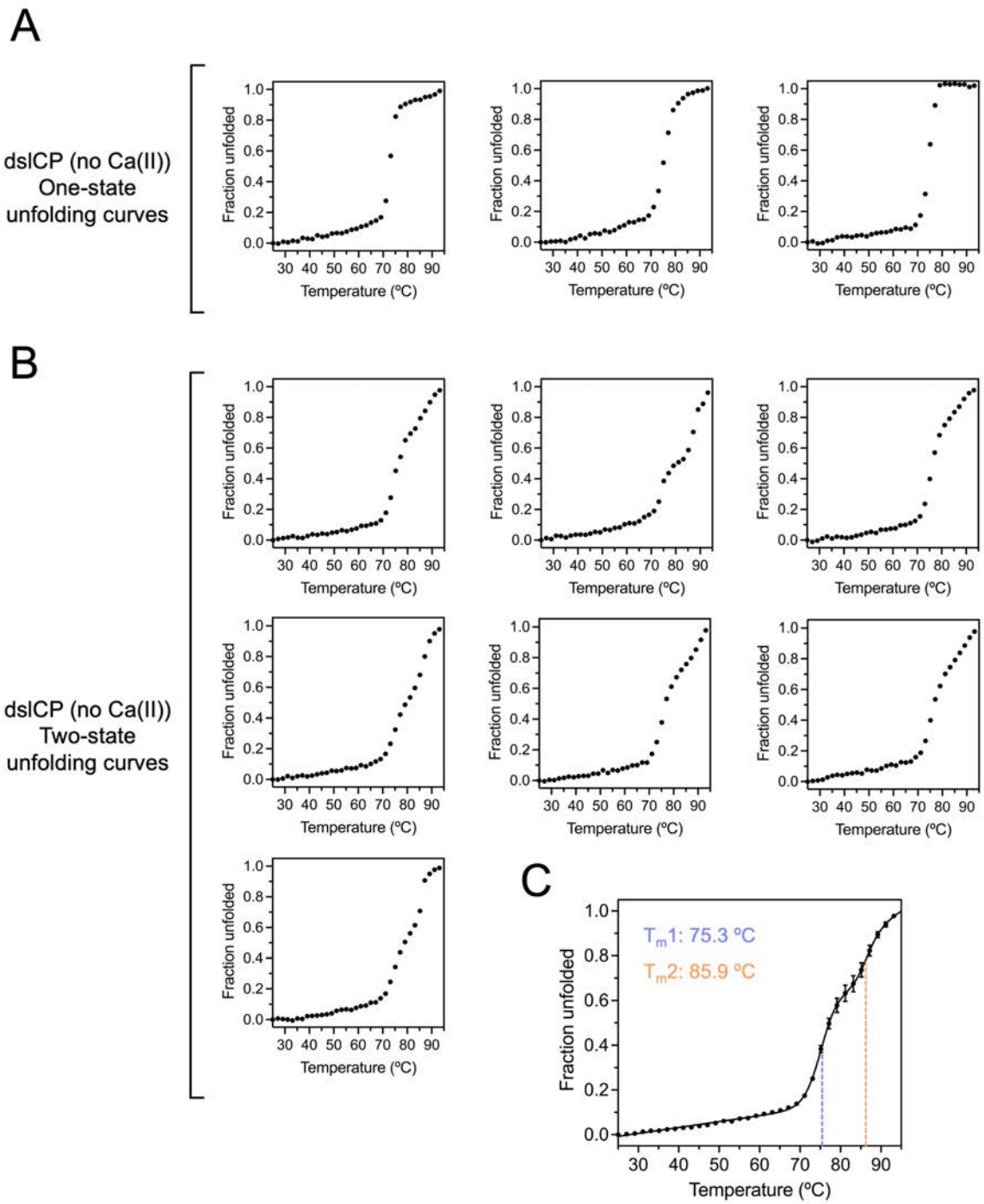

Figure S11. Ten independent replicates of dslCP thermal denaturation in the absence of added Ca(II). (A) The top three replicates display what appears to be a single melting transition, whereas (B) the bottom seven exhibit a non-singular transition. Thermal denaturation curves were recorded by monitoring the absorption at 222 nm for 10 μM protein in 1 mM Tris pH 7.5 buffer with a 2-ºC/min ramp rate. (C) The seven replicates with non-singular transitions were averaged, and values are reported as mean ± s.e.m. (*n* = 7). The data points were fitted to a two-transition Boltzmann sigmoidal model (see Equation 2 in the Methods section), shown as a solid line. The extracted T_m values are reported on the plot.

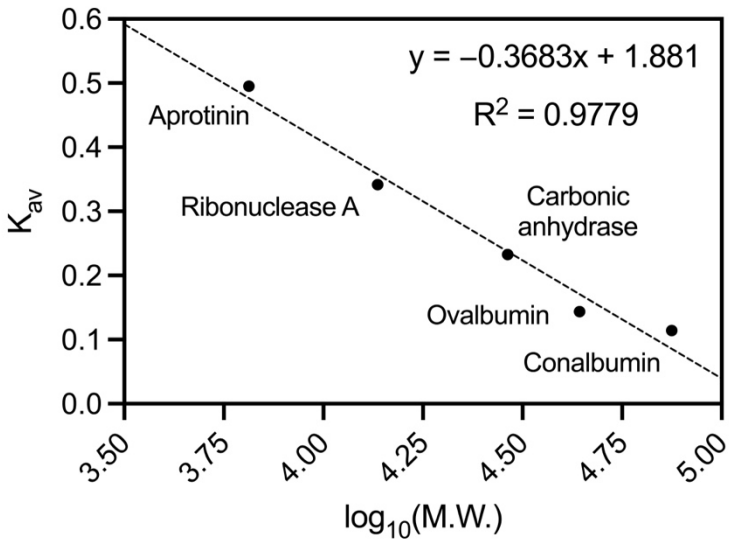

Figure S12. Standard curve for SEC molecular weight calculations. Proteins used for the standard curve are indicated on the plot. Aprotinin: 6.5 kDa, ribonuclease A: 13.7 kDa, carbonic anhydrase: 29 kDa, ovalbumin: 43 kDa, conalbumin: 75 kDa.

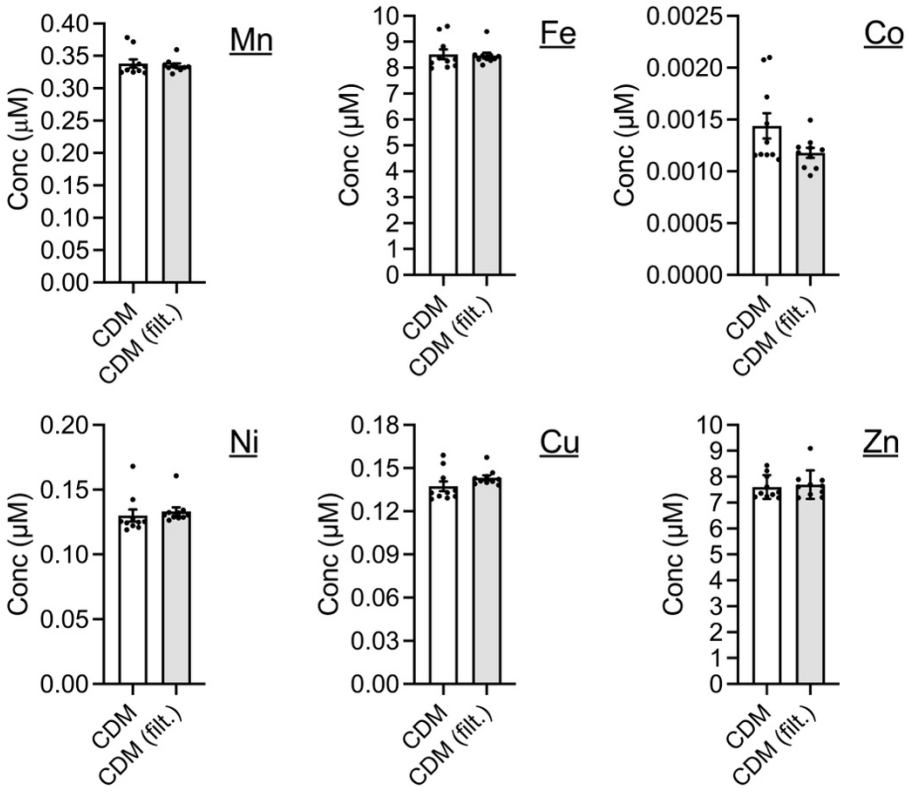

Figure S13. Metal content of filtered and unfiltered CDM corresponding to the metal-depletion experiment in **Figure 4** (main text). CDM was incubated for 24 h at 30 ºC with shaking (150 rpm) in the absence of protein. Metal content was quantified by ICP-MS either directly or following filtration through a 10-kDa molecular weight cutoff filter. All values are reported as mean ± s.e.m.; *n* = 10 for all samples.

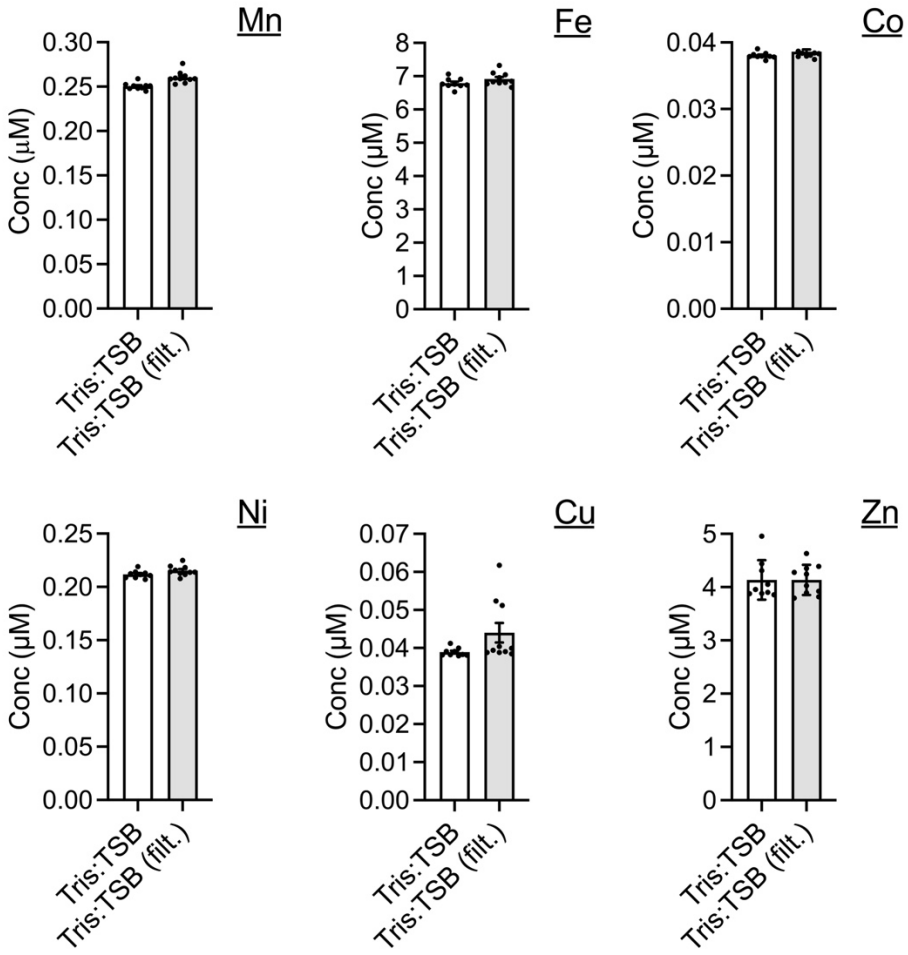

Figure S14. Metal content of filtered and unfiltered Tris:TSB corresponding to the metal-depletion experiment in **Figure 4** (main text). Tris:TSB was incubated for 24 h at 30 ºC with shaking (150 rpm) in the absence of protein. Metal content was quantified by ICP-MS either directly or following filtration through a 10-kDa molecular weight cutoff filter. All values are reported as mean ± s.e.m.; *n* = 10 for all samples.

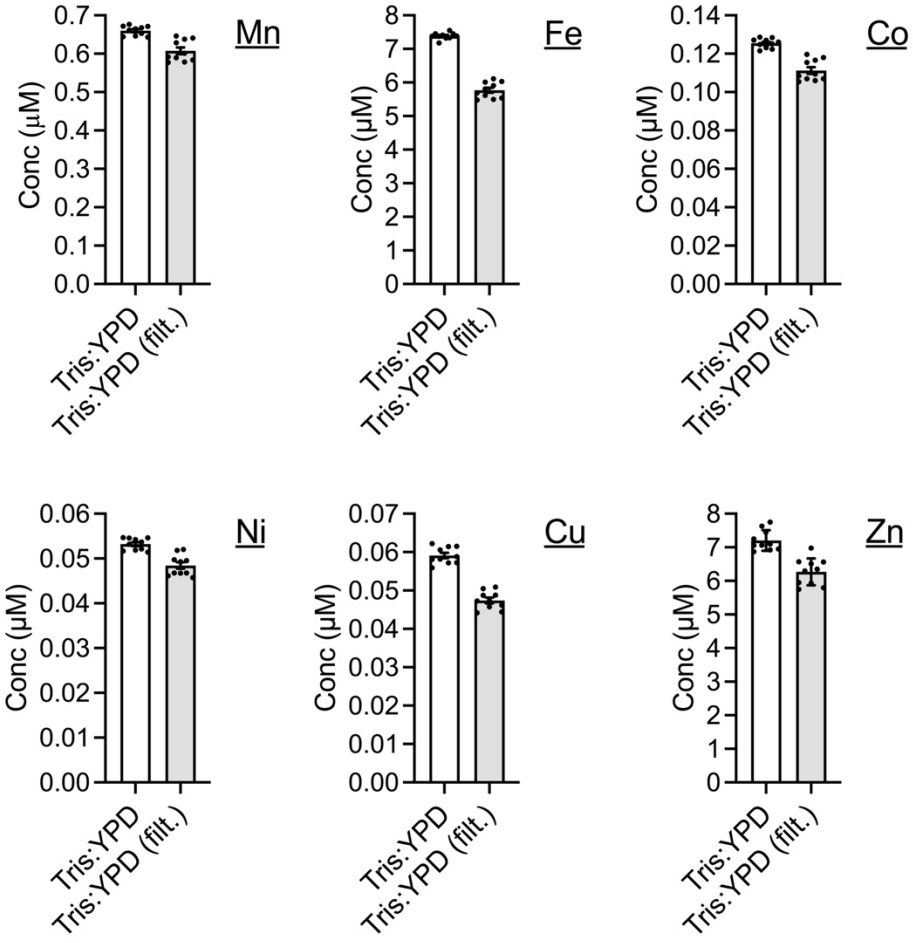

Figure S15. Metal content of filtered and unfiltered Tris:YPD corresponding to the metal-depletion experiment in **Figure 4** (main text). Tris:YPD was incubated for 24 h at 30 ºC with shaking (150 rpm) in the absence of protein. Metal content was quantified by ICP-MS either directly or following filtration through a 10-kDa molecular weight cutoff filter. All values are reported as mean ± s.e.m.; *n* = 10 for all samples.

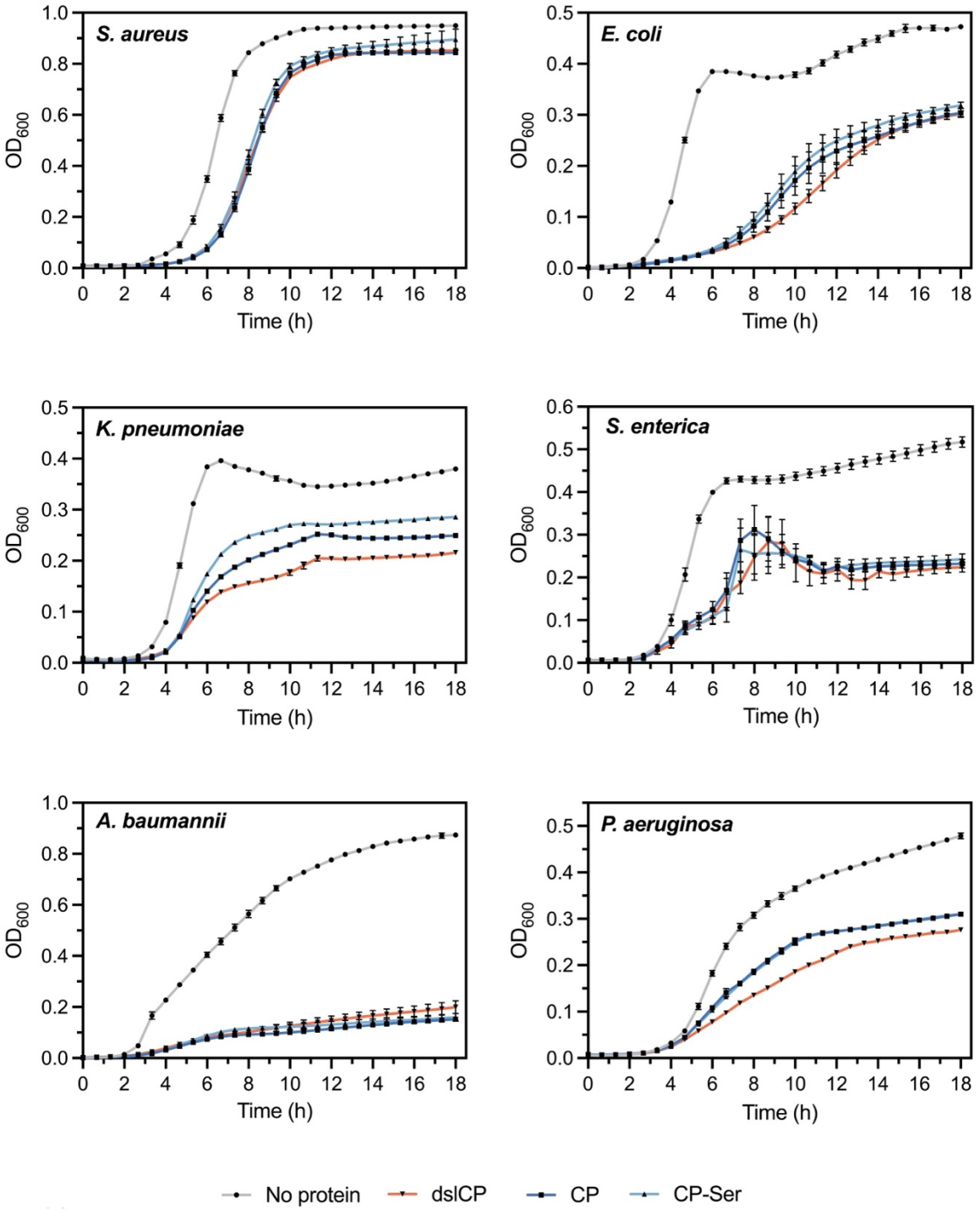

Figure S16. Antimicrobial activity of dslCP, CP and CP-Ser against *S. aureus* USA300 JE2, *E. coli* CFT073, *K. pneumoniae* ATCC 13883, *S. enterica* IR715, *A. baumannii* ATCC 17978 and *P. aeruginosa* PA14 grown in CDM. The medium was supplemented with ± 10 μM protein and growth was monitored over 18 h at 37 ºC and 700 rpm in a 96-well plate, with OD_{600} measurements every 40 min. Curves represent the mean of 6 biological replicates (each the average of 3 technical replicates); error bars indicate s.e.m. across biological replicates (for *S. enterica*, *n* = 9).

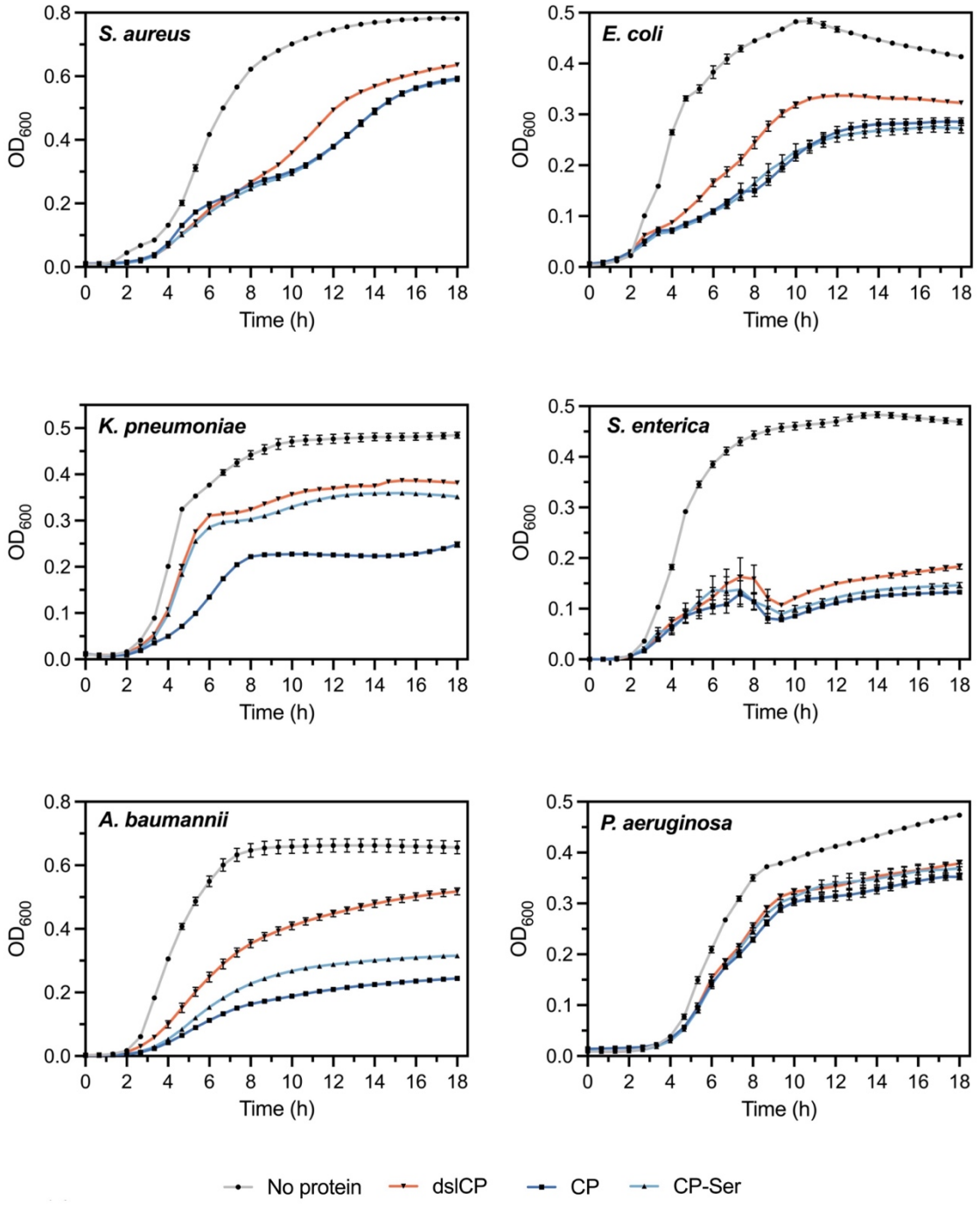

Figure S17. Antimicrobial activity of dslCP, CP and CP-Ser against *S. aureus* USA300 JE2, *E. coli* CFT073, *K. pneumoniae* ATCC 13883, *S. enterica* IR715, *A. baumannii* ATCC 17978 and *P. aeruginosa* PA14 grown in Tris:TSB. The medium was supplemented with ± 10 μM protein and growth was monitored over 18 h at 37 ºC and 700 rpm in a 96-well plate, with OD_{600} measurements every 40 min. Curves represent the mean of 6 biological replicates (each the average of 3 technical replicates); error bars indicate s.e.m. across biological replicates (for *S. enterica*, $n = 9$).

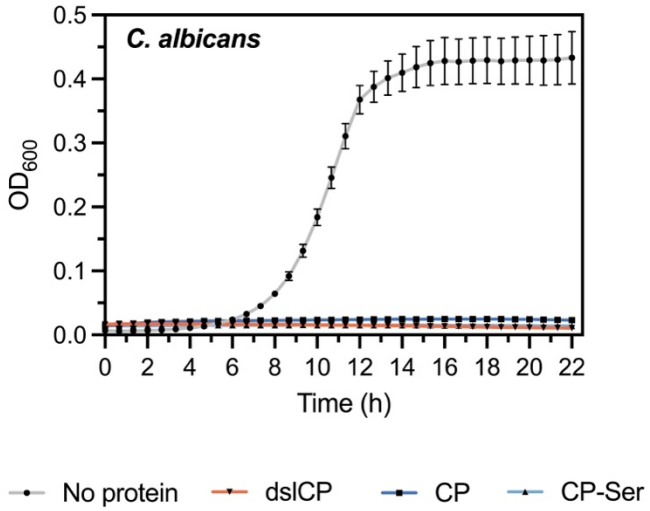

Figure S18. Antimicrobial activity of dslCP, CP and CP-Ser against *C. albicans* SC5314 grown in Tris:YPD. The medium was supplemented with ± 10 μM protein and growth was monitored over 22 h at 37 ºC and 800 rpm in a 96-well plate, with OD_{600} measurements every 40 min. Curves represent the mean of 6 biological replicates (each the average of 3 technical replicates); error bars indicate s.e.m. across biological replicates.

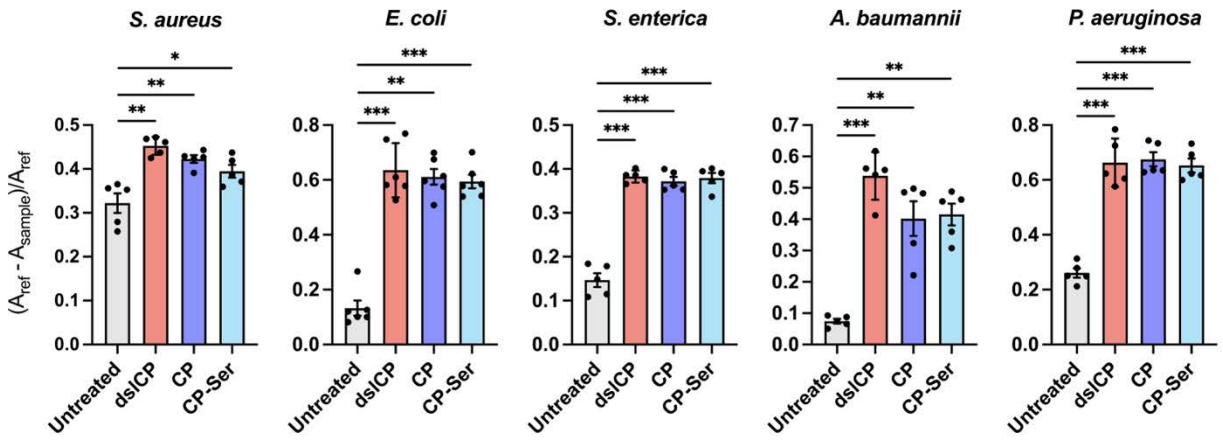

Figure S19. Unnormalized siderophore content of bacterial supernatants following 8 h of growth at 37 °C in CDM with dslCP, CP or CP-Ser treatment. A_{ref} is the reference containing only medium and dye solution and A_{sample} is the absorbance of the sample at 630 nm. The unnormalized values are based solely on the plate readouts; see the Methods section for details on the dilutions used for each organism and the normalization method used for the figure in the main text. All values are reported as mean ± s.e.m.; $n = 5$ for all samples except *E. coli* ($n = 6$). Statistical significance was assessed by pairwise comparisons (Welch's two-sample *t*-test) between each individual treatment group and the untreated control. No statistical comparisons were made between different protein treatment groups. * $p < 0.05$, ** $p < 0.01$, *** $p < 0.001$.

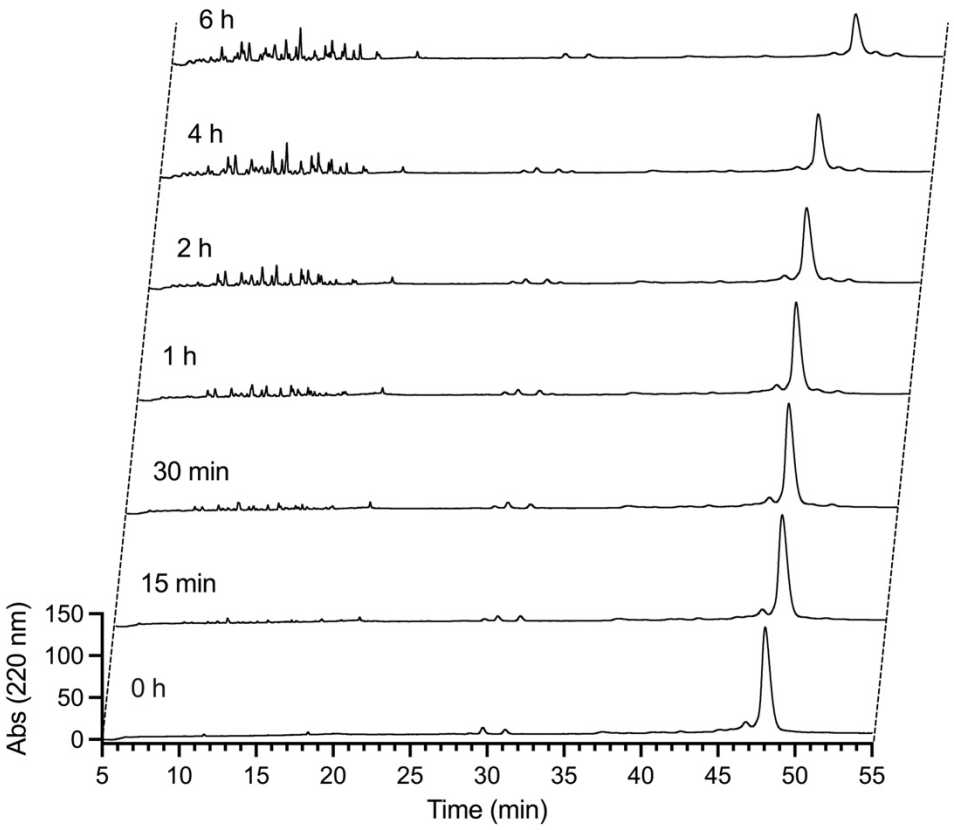

Figure S20. Representative full HPLC time-course stack plot for dslCP (30 μM) treated with 2.5 μM HNE for 0–6 h in the presence of 3 mM Ca(II).

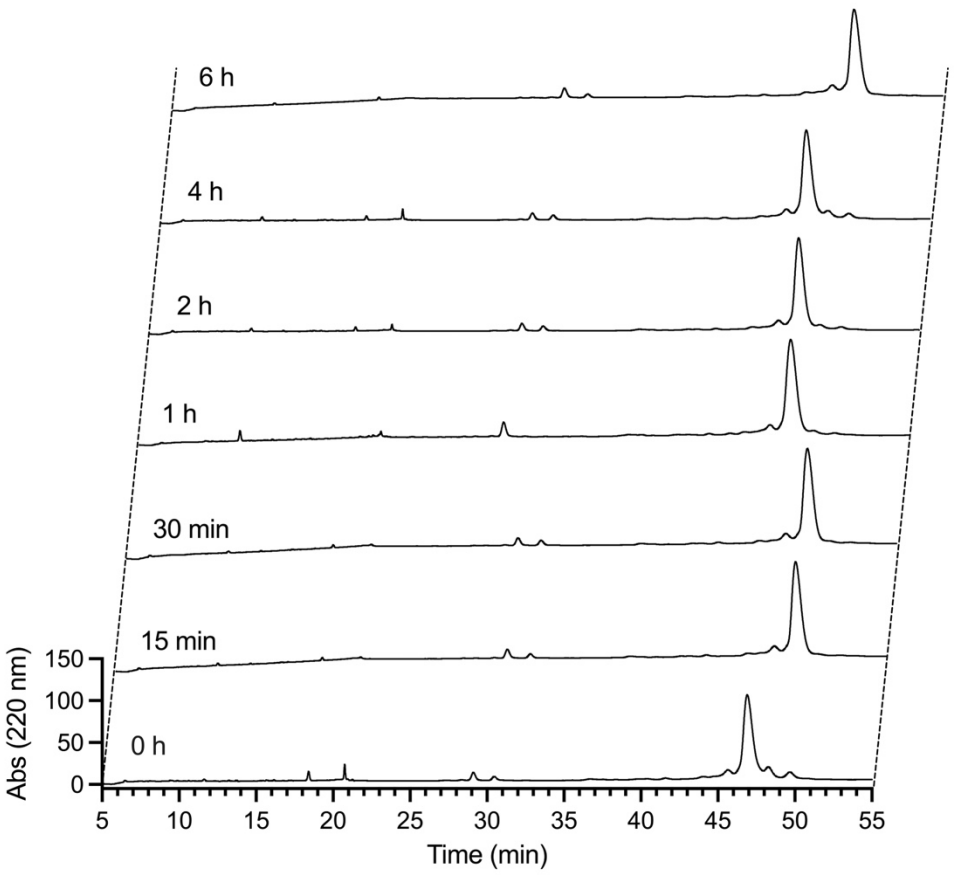

Figure S21. Representative full HPLC time-course stack plot for dslCP (30 μM) treated with 2.5 μM HNE for 0–6 h in the presence of 3 mM Ca(II) and 1 equiv Mn(II).

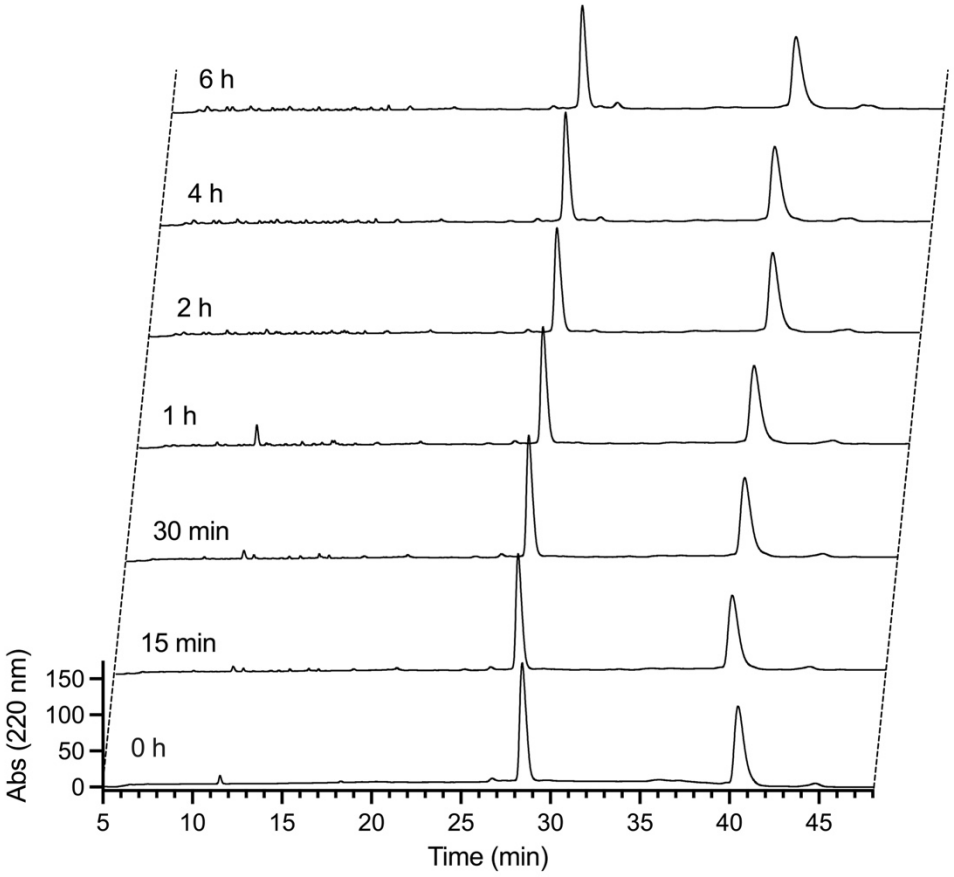

Figure S22. Representative full HPLC time-course stack plot for CP-Ser (30 μM) treated with 2.5 μM HNE for 0–6 h in the presence of 3 mM Ca(II).

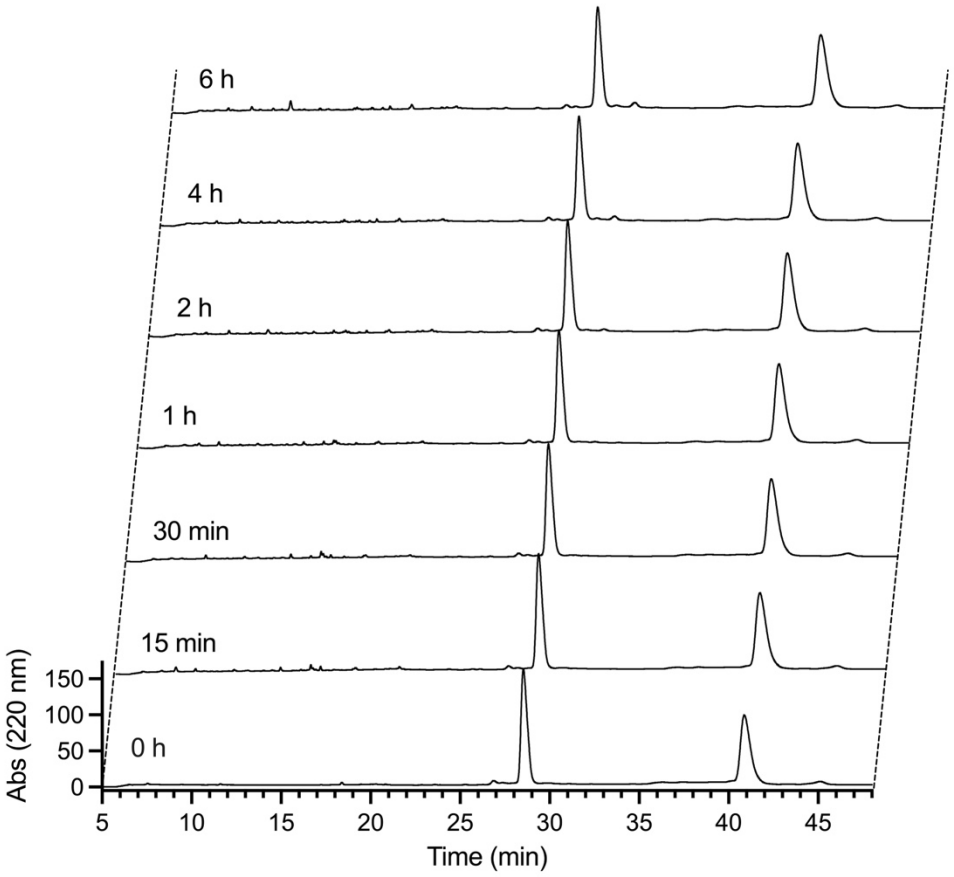

Figure S23. Representative full HPLC time-course stack plot for CP-Ser (30 μM) treated with 2.5 μM HNE for 0–6 h in the presence of 3 mM Ca(II) and 1 equiv Mn(II).

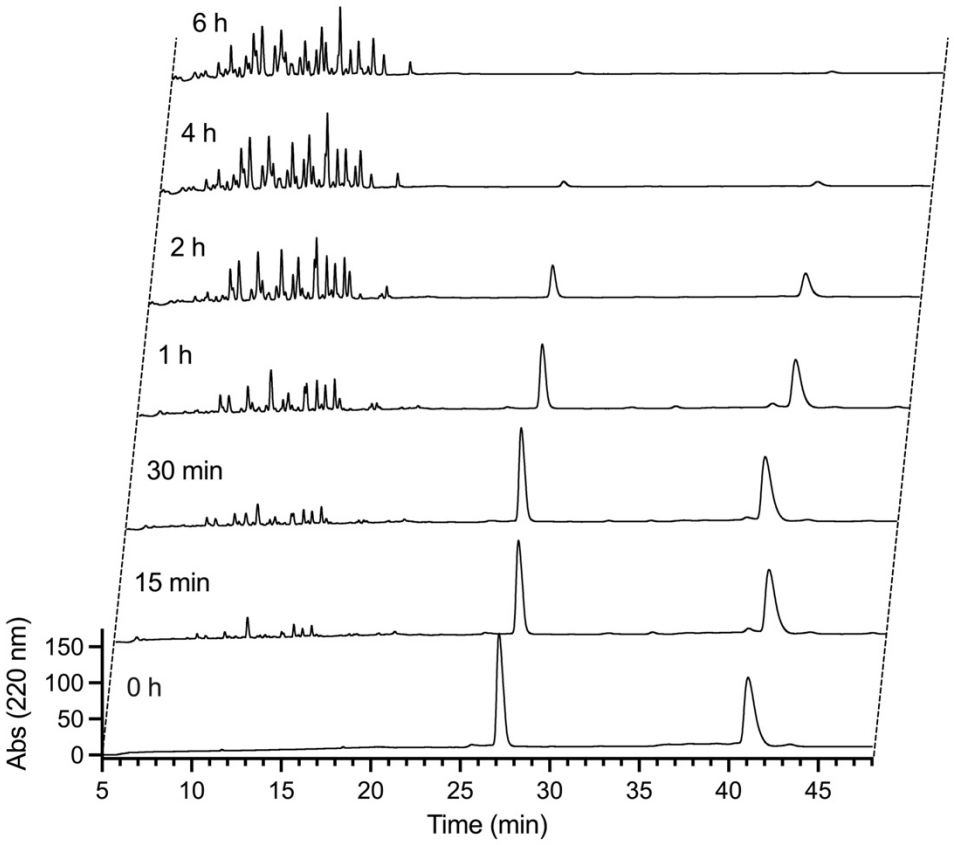

Figure S24. Representative full HPLC time-course stack plot for CP-Ser^{I60E} (30 μM) treated with 2.5 μM HNE for 0–6 h in the presence of 3 mM Ca(II).

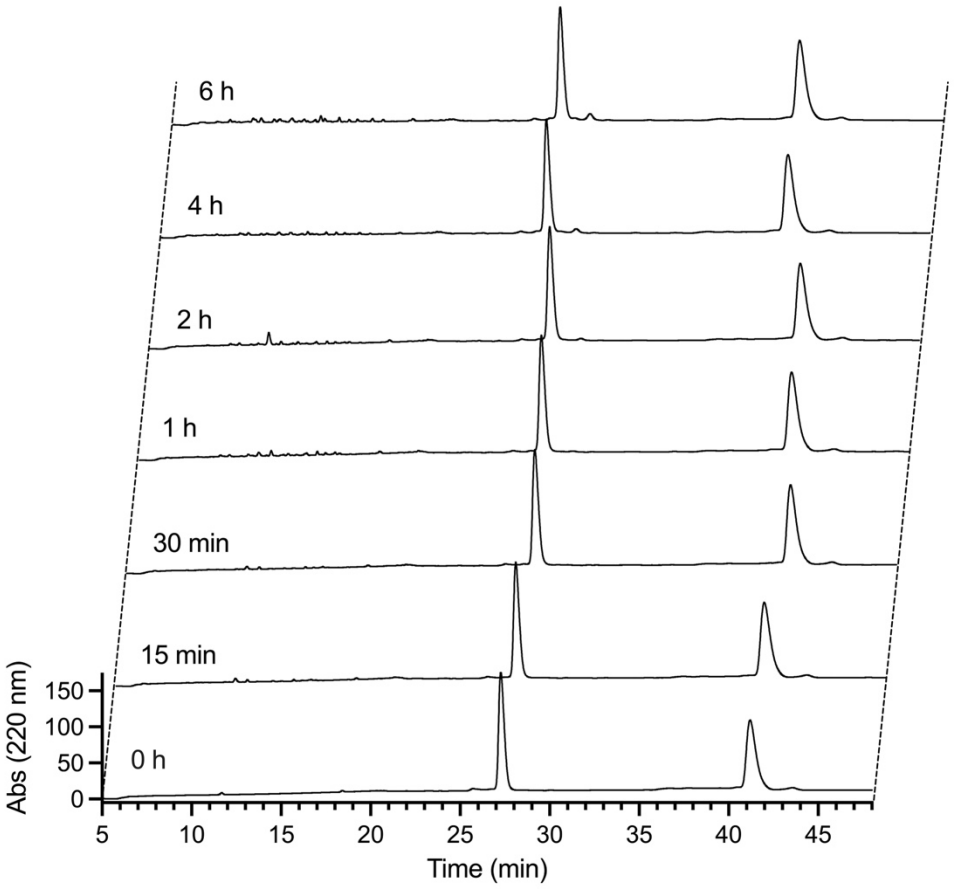

Figure S25. Representative full HPLC time-course stack plot for CP-Ser^{I60E} (30 μM) treated with 2.5 μM HNE for 0–6 h in the presence of 3 mM Ca(II) and 1 equiv Mn(II).

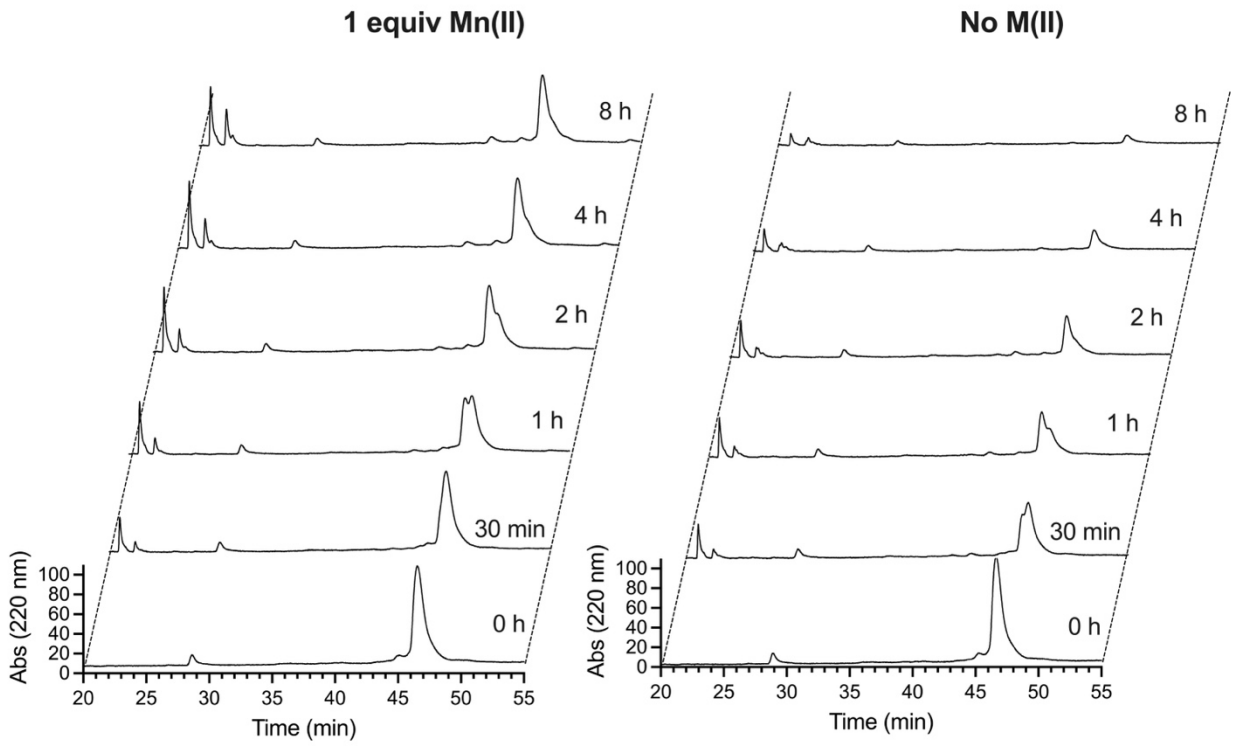

Figure S26. Representative full HPLC time-course stack plots for dslCP (30 μM) treated with 1 μM trypsin for 0–8 h in the presence (left) and absence (right) of 1 equiv Mn(II), with 3 mM Ca(II) present in all samples.

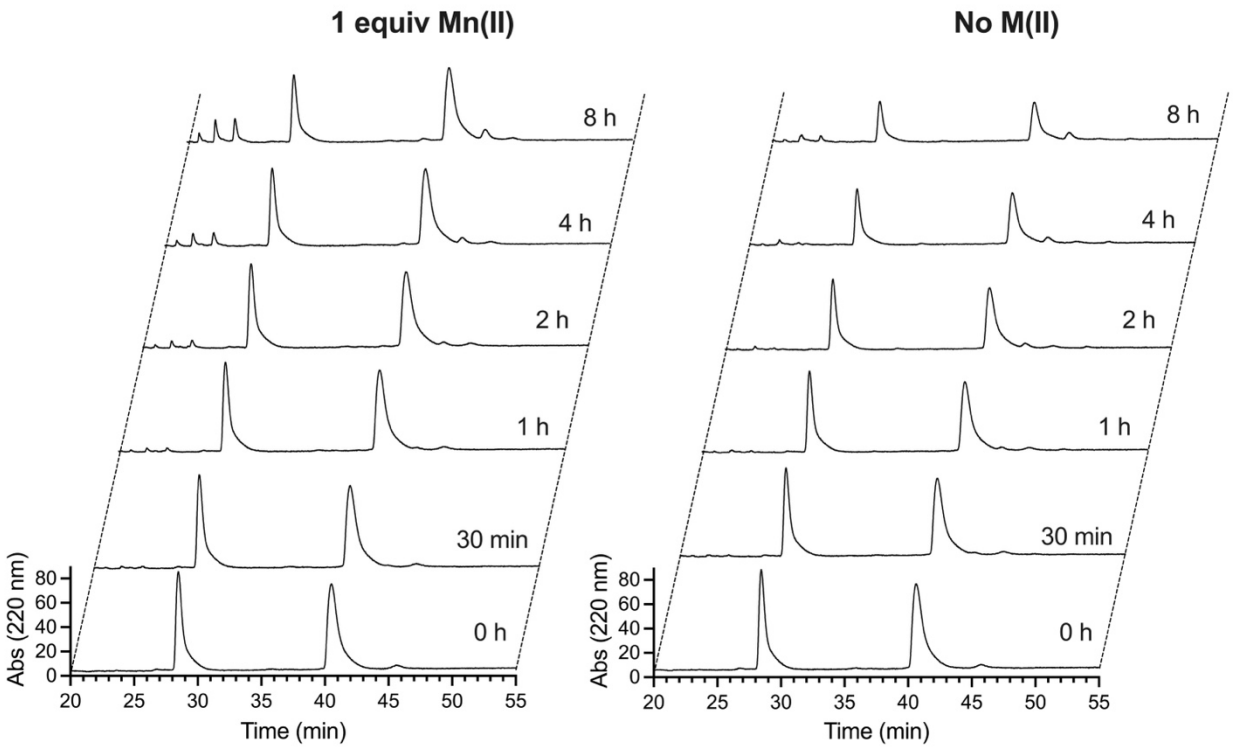

Figure S27. Representative full HPLC time-course stack plots for CP-Ser (30 μM) treated with 1 μM trypsin for 0–8 h in the presence (left) and absence (right) of 1 equiv Mn(II), with 3 mM Ca(II) present in all samples.

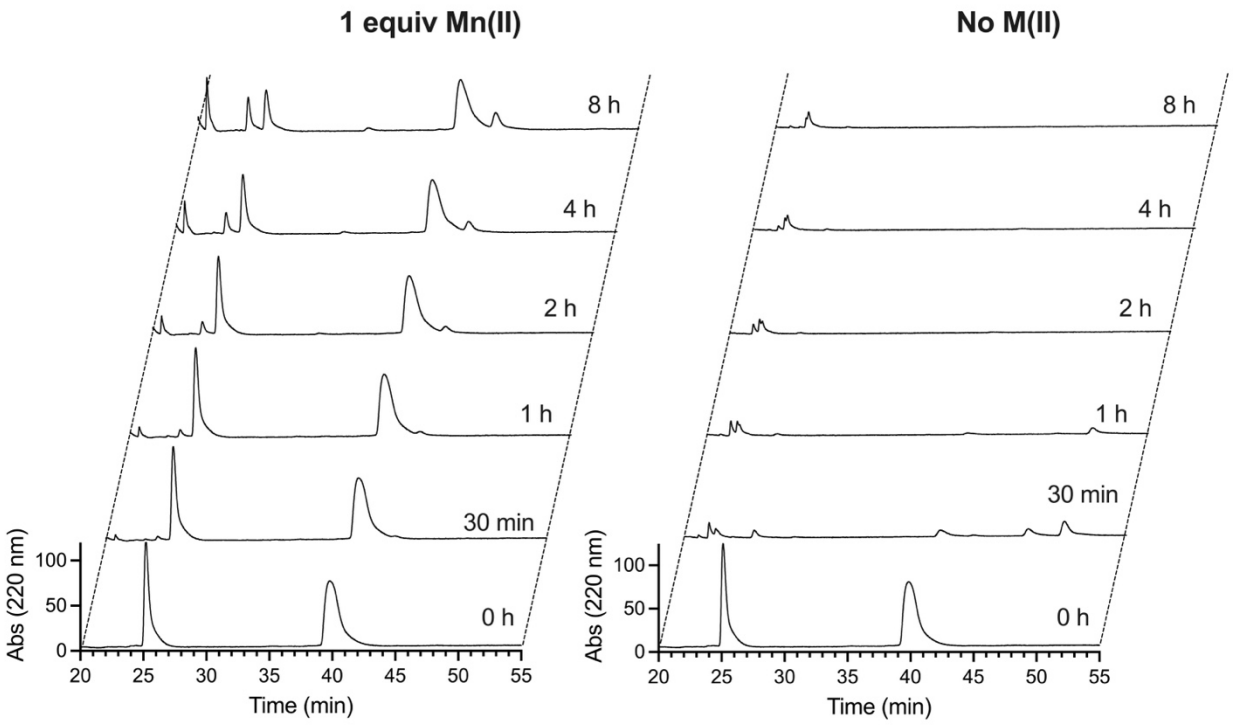

Figure S28. Representative full HPLC time-course stack plots for CP-Ser^{I60E} (30 μM) treated with 1 μM trypsin for 0–8 h in the presence (left) and absence (right) of 1 equiv Mn(II), with 3 mM Ca(II) present in all samples.

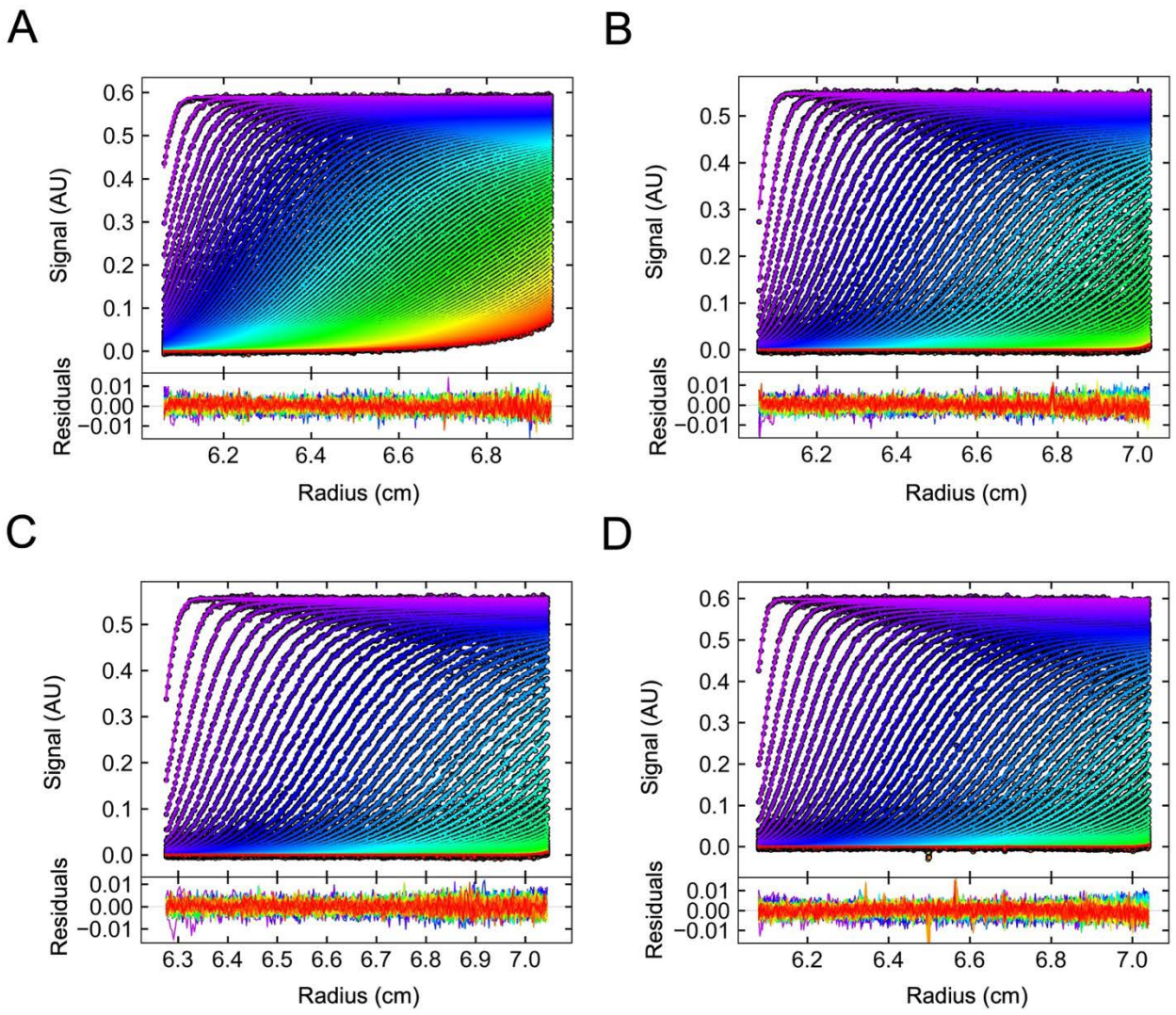

Figure S29. Sedimentation boundaries and residuals for dsICP (27.5 μM) analyzed by sedimentation velocity analytical ultracentrifugation (SV-AUC), replicate #1. (A) Apo protein. (B) Protein + 550 μM Ca(II). (C) Protein + 2 mM Ca(II). (D) Protein + 550 μM Ca(II) + 27.5 μM Mn(II). All samples were analyzed in 75 mM HEPES (pH 7.5), 100 mM NaCl. Experimental data (black points) are shown with fitted curves (colored lines); residuals are displayed below each boundary plot. Fitting parameters and derived results are reported in **Tables S11** and **S12**, respectively.

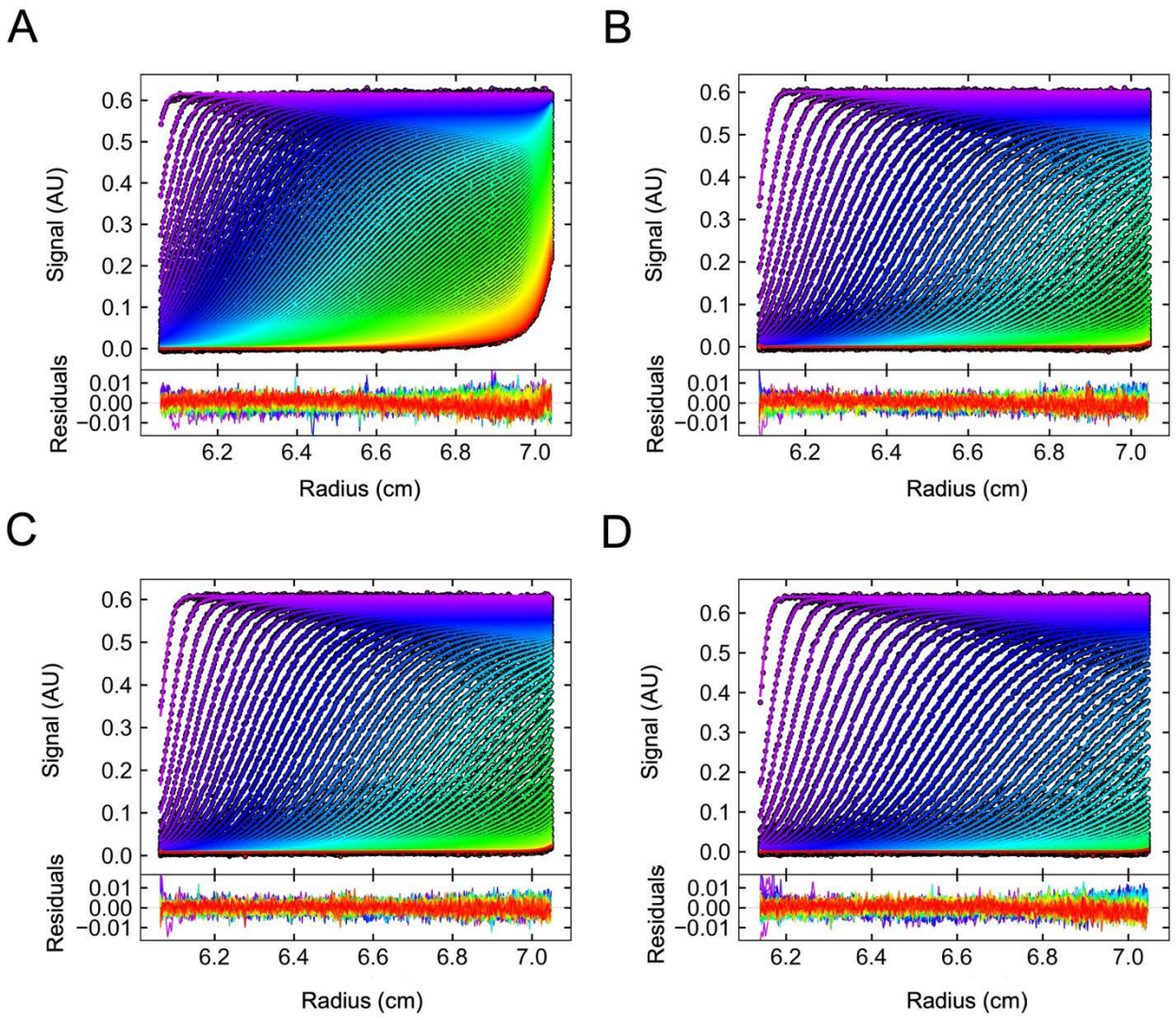

Figure S30. Sedimentation boundaries and residuals for CP-Ser (27.5 μM) analyzed by sedimentation velocity analytical ultracentrifugation (SV-AUC), replicate #1. (A) Apo protein. (B) Protein + 550 μM Ca(II). (C) Protein + 2 mM Ca(II). (D) Protein + 550 μM Ca(II) + 27.5 μM Mn(II). All samples were analyzed in 75 mM HEPES (pH 7.5), 100 mM NaCl. Experimental data (black points) are shown with fitted curves (colored lines); residuals are displayed below each boundary plot. Fitting parameters and derived results are reported in **Tables S11** and **S12**, respectively.

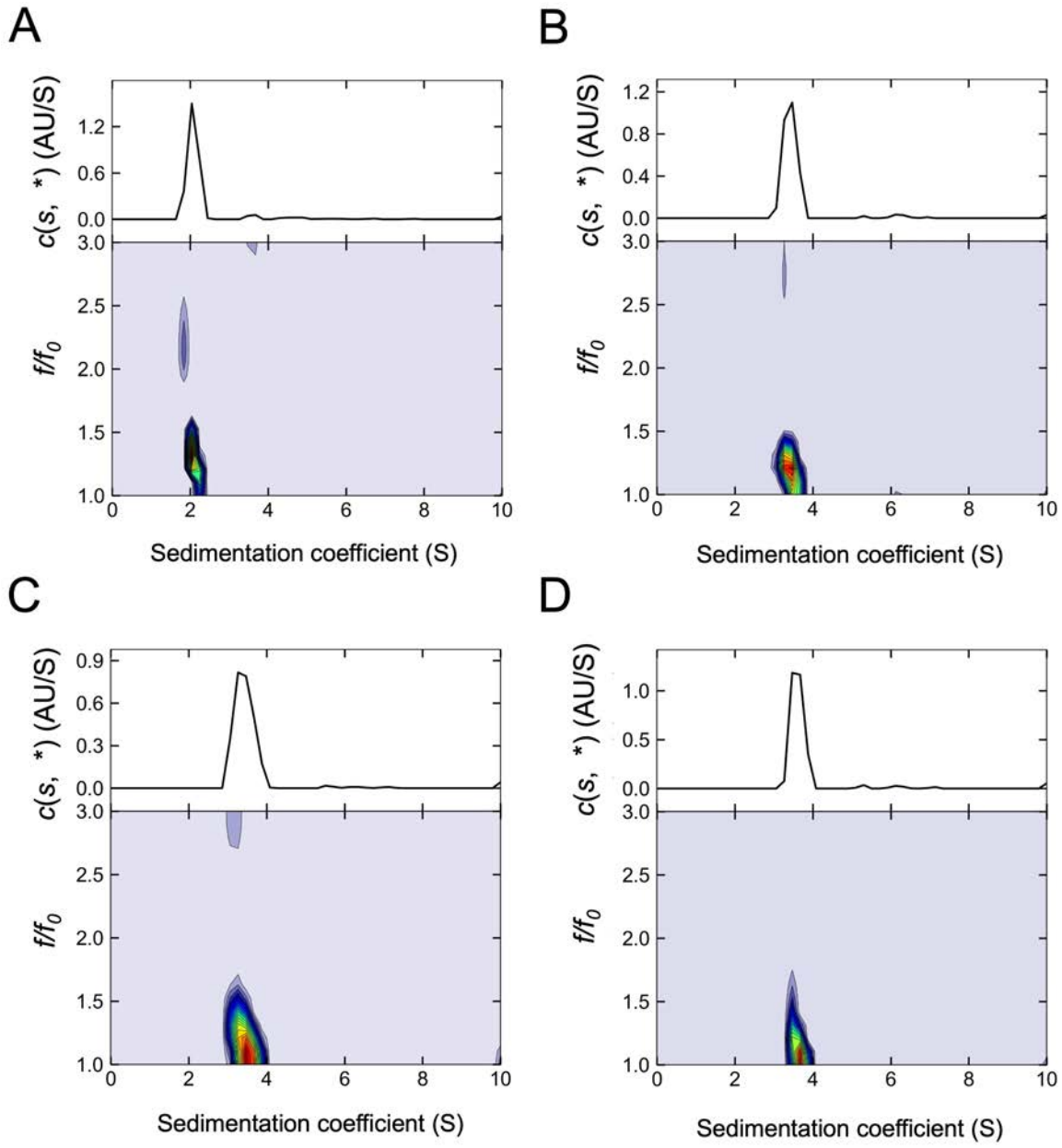

Figure S31. Two-dimensional $c(S)–f/f_0$ distributions for dslCP (27.5 μM) obtained by sedimentation velocity analytical ultracentrifugation (SV-AUC), replicate #1. Each panel shows the sedimentation-coefficient distribution $c(S, f/f_0)$ (lower contour plot) and the corresponding one-dimensional $c(S)$ projection (upper trace). The frictional ratio (f/f_0) describes the deviation from an ideal spherical shape; lower f/f_0 values indicate a more compact, globular protein, whereas higher values reflect an elongated or partially unfolded conformation. Sedimentation coefficients were corrected for water and 20 ºC ($S_{20,w}$). (A) Apo protein. (B) Protein + 550 μM Ca(II). (C) Protein + 2 mM Ca(II). (D) Protein + 550 μM Ca(II) + 27.5 μM Mn(II). All samples were analyzed in 75 mM HEPES (pH 7.5), 100 mM NaCl. Fitting parameters and derived results are reported in **Tables S11** and **S13**, respectively.

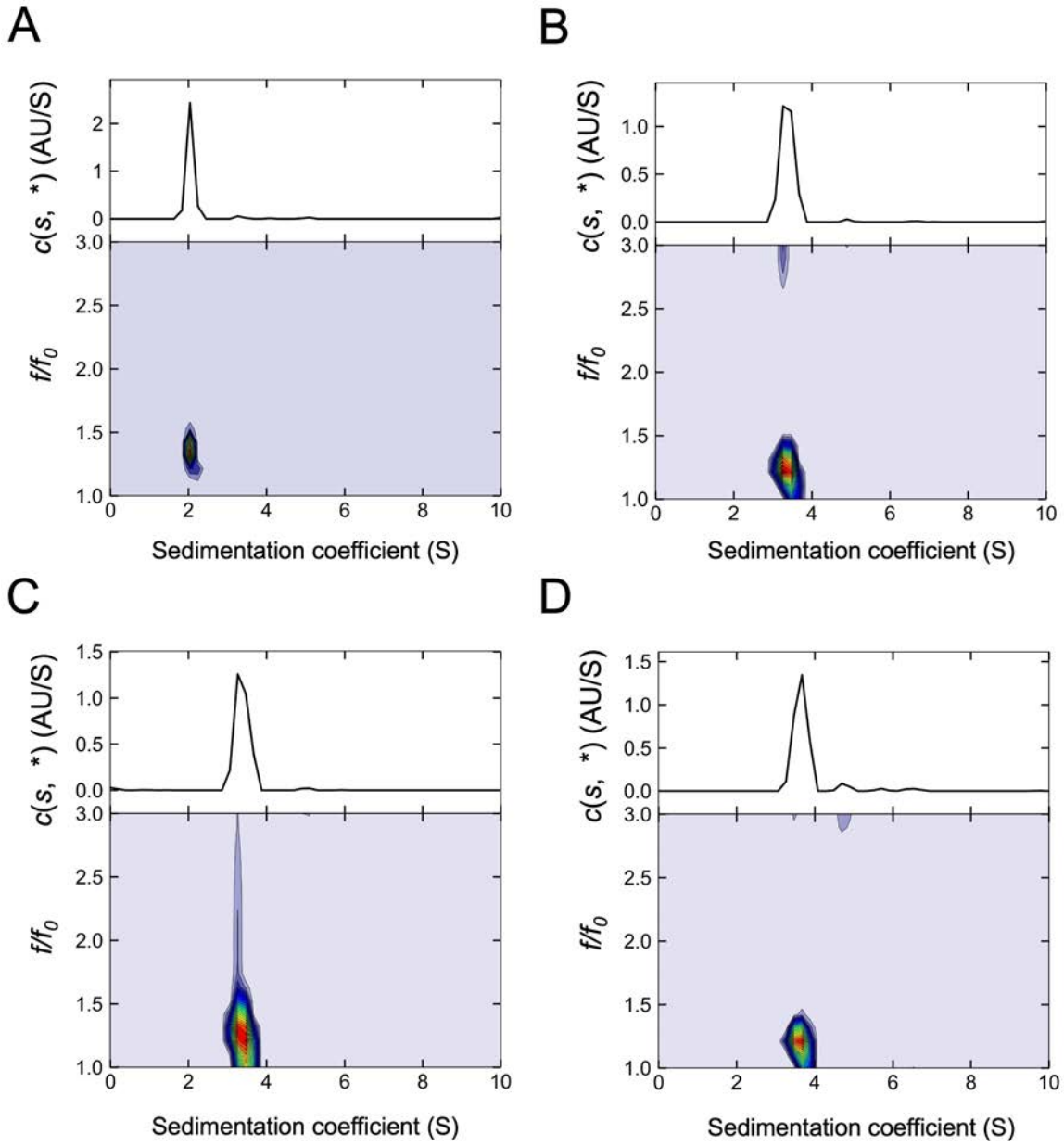

Figure S32. Two-dimensional $c(S)–f/f_0$ distributions for CP-Ser (27.5 μM) obtained by sedimentation velocity analytical ultracentrifugation (SV-AUC), replicate #1. Each panel shows the sedimentation-coefficient distribution $c(S, f/f_0)$ (lower contour plot) and the corresponding one-dimensional $c(S)$ projection (upper trace). The frictional ratio (f/f_0) describes the deviation from an ideal spherical shape; lower f/f_0 values indicate a more compact, globular protein, whereas higher values reflect an elongated or partially unfolded conformation. Sedimentation coefficients were corrected for water and 20 ºC ($S_{20,w}$). (A) Apo protein. (B) Protein + 550 μM Ca(II). (C) Protein + 2 mM Ca(II). (D) Protein + 550 μM Ca(II) + 27.5 μM Mn(II). All samples were analyzed in 75 mM HEPES (pH 7.5), 100 mM NaCl. Fitting parameters and derived results are reported in **Tables S11** and **S13**, respectively.

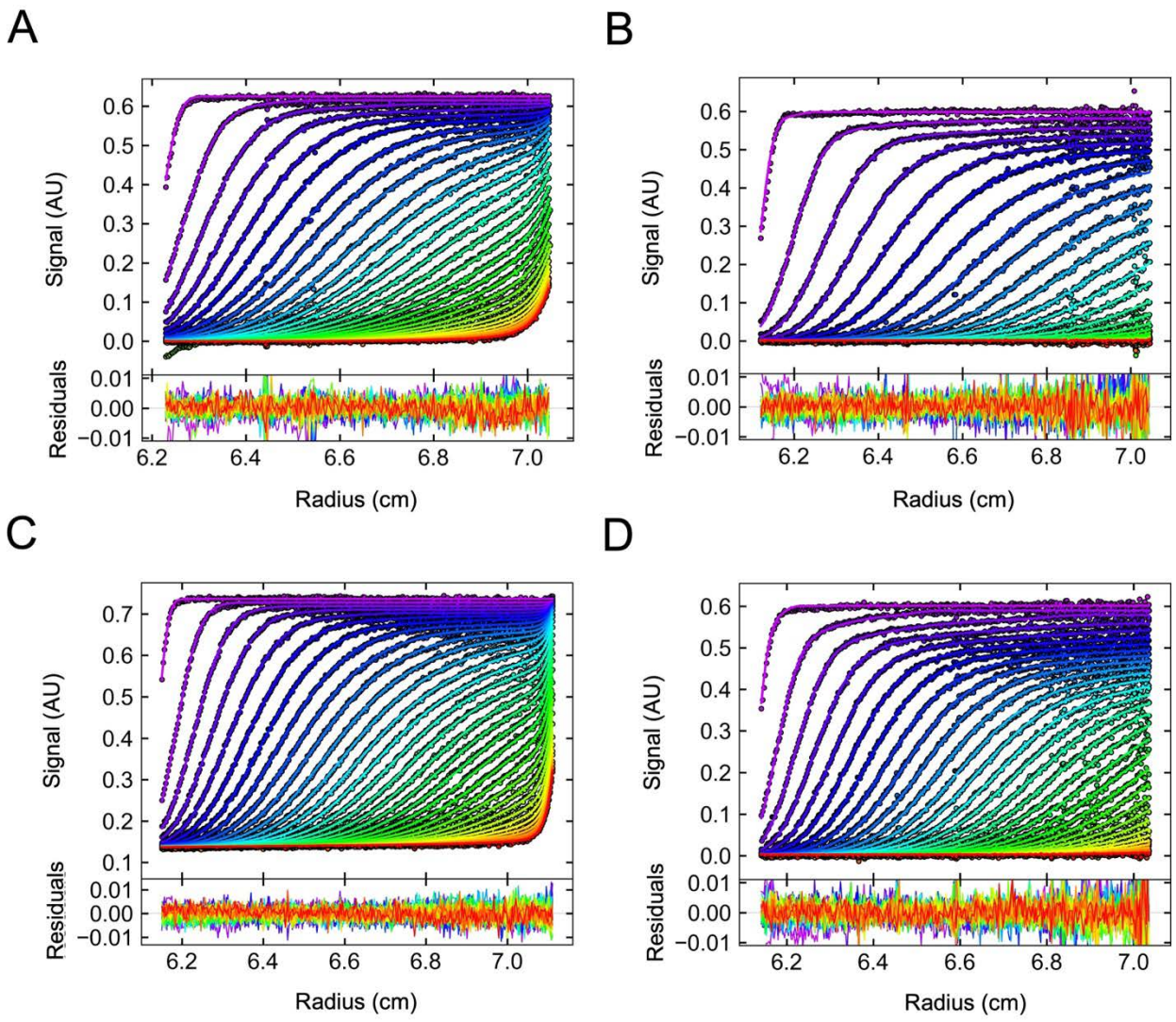

Figure S33. Sedimentation boundaries and residuals for dslCP (27.5 μM) analyzed by sedimentation velocity analytical ultracentrifugation (SV-AUC), replicate #2. (A) Apo protein. (B) Protein + 550 μM Ca(II). (C) Protein + 2 mM Ca(II). (D) Protein + 550 μM Ca(II) + 27.5 μM Mn(II). All samples were analyzed in 75 mM HEPES (pH 7.5), 100 mM NaCl. Experimental data (black points) are shown with fitted curves (colored lines); residuals are displayed below each boundary plot. Fitting parameters and derived results are reported in **Tables S11** and **S12**, respectively.

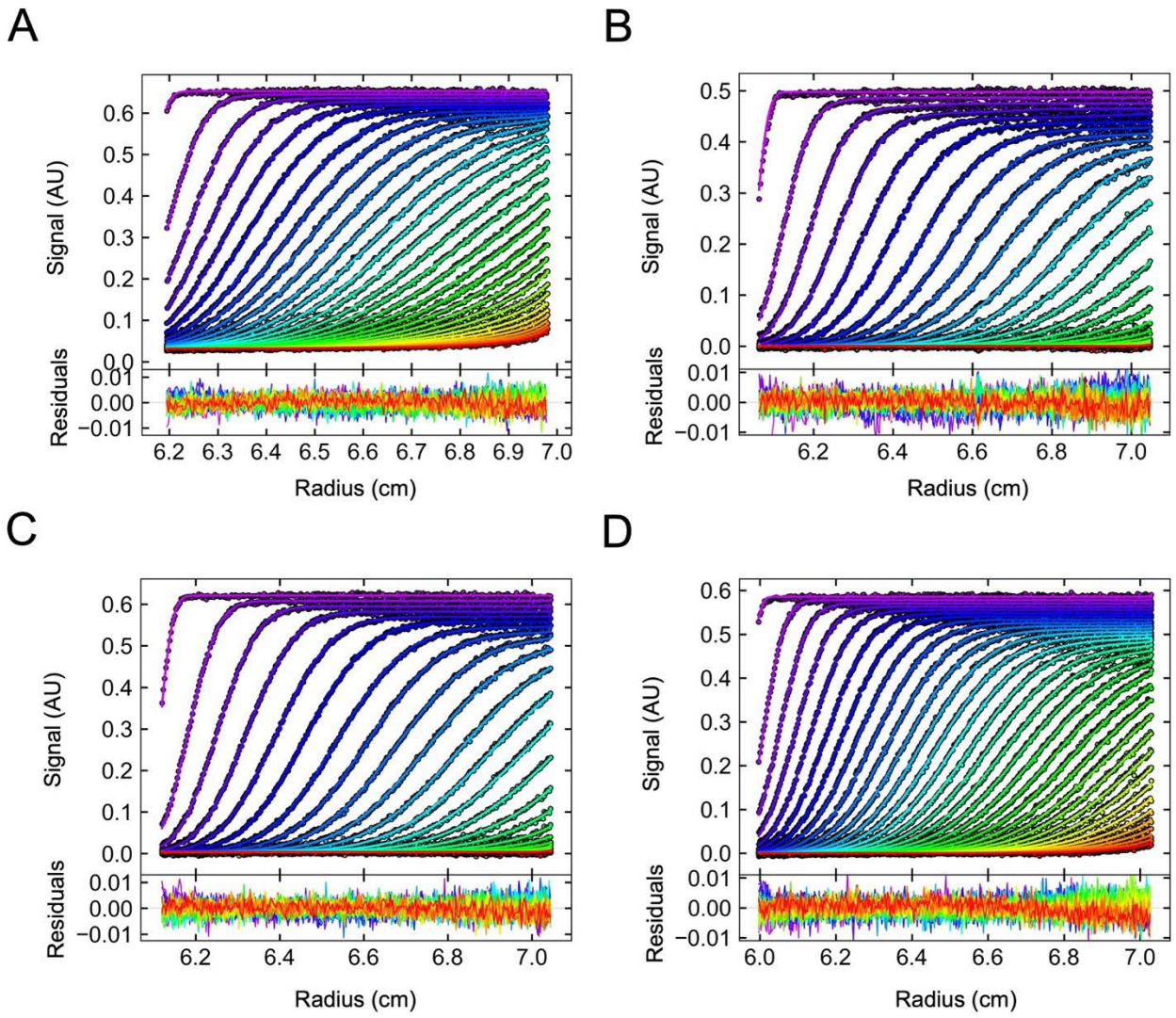

Figure S34. Sedimentation boundaries and residuals for CP-Ser (27.5 μM) analyzed by sedimentation velocity analytical ultracentrifugation (SV-AUC), replicate #2. (A) Apo protein. (B) Protein + 550 μM Ca(II). (C) Protein + 2 mM Ca(II). (D) Protein + 550 μM Ca(II) + 27.5 μM Mn(II). All samples were analyzed in 75 mM HEPES (pH 7.5), 100 mM NaCl. Experimental data (black points) are shown with fitted curves (colored lines); residuals are displayed below each boundary plot. Fitting parameters and derived results are reported in **Tables S11** and **S12**, respectively.

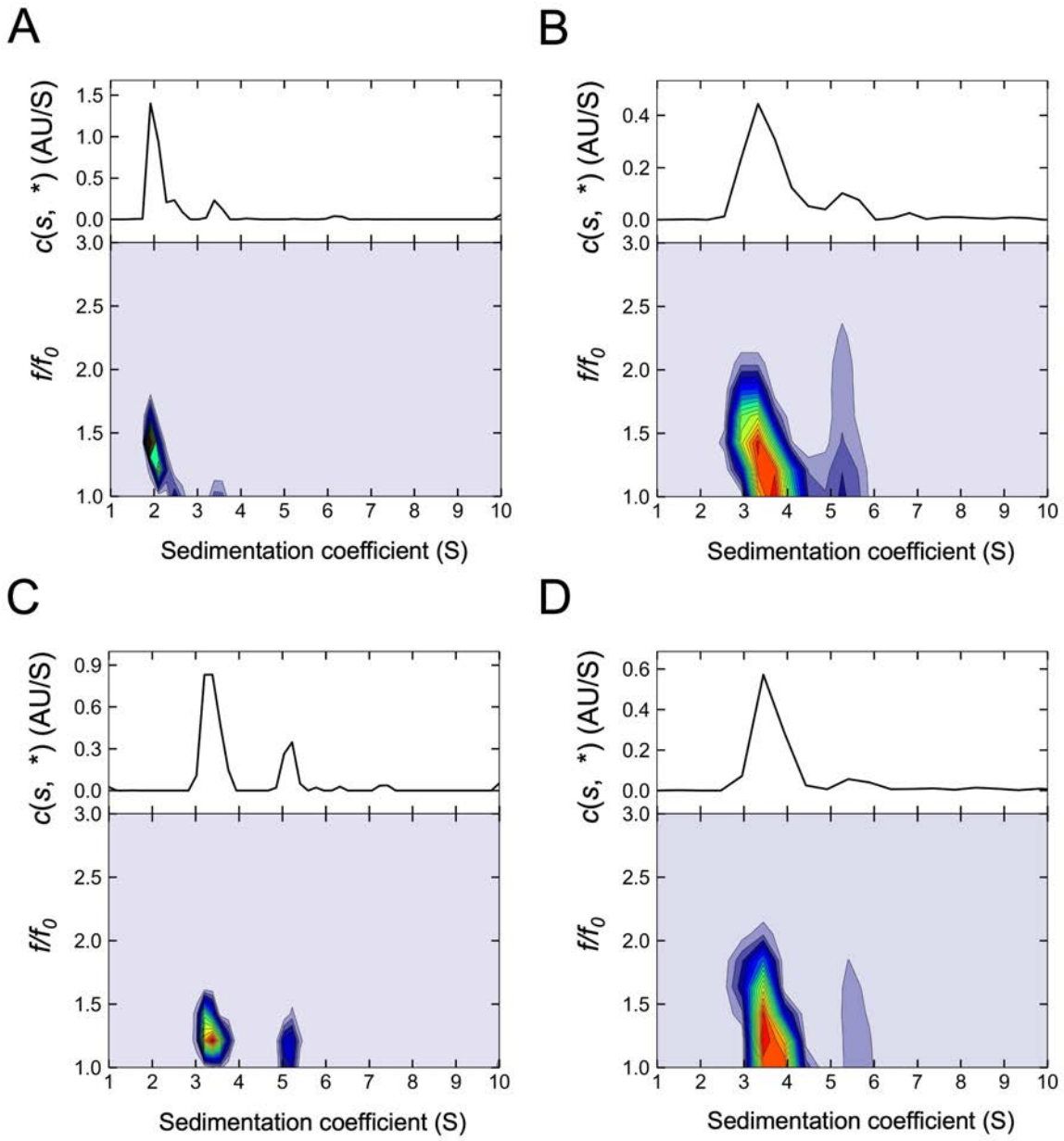

Figure S35. Two-dimensional *c(S)–f/f₀* distributions for dsICP (27.5 μM) obtained by sedimentation velocity analytical ultracentrifugation (SV-AUC), replicate #2. Each panel shows the sedimentation-coefficient distribution *c(S, f/f₀)* (lower contour plot) and the corresponding one-dimensional *c(S)* projection (upper trace). The frictional ratio (*f/f₀*) describes the deviation from an ideal spherical shape; lower *f/f₀* values indicate a more compact, globular protein, whereas higher values reflect an elongated or partially unfolded conformation. Sedimentation coefficients were corrected for water and 20 ºC ($S_{20,w}$). (A) Apo protein. (B) Protein + 550 μM Ca(II). (C) Protein + 2 mM Ca(II). (D) Protein + 550 μM Ca(II) + 27.5 μM Mn(II). All samples were analyzed in 75 mM HEPES (pH 7.5), 100 mM NaCl. Fitting parameters and derived results are reported in **Tables S11** and **S13**, respectively.

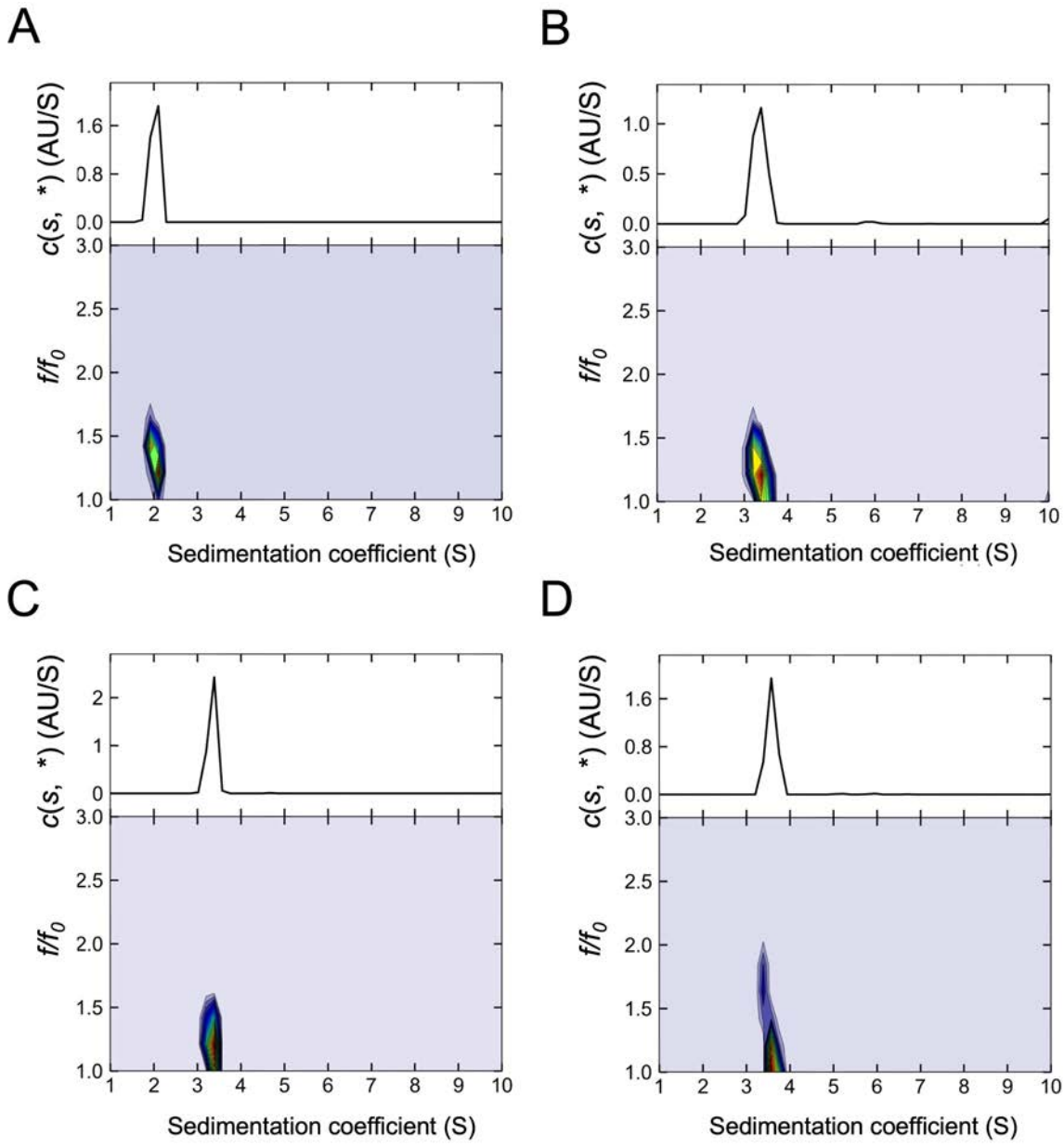

Figure S36. Two-dimensional *c(S)–f/f₀* distributions for CP-Ser (27.5 μM) obtained by sedimentation velocity analytical ultracentrifugation (SV-AUC), replicate #2. Each panel shows the sedimentation-coefficient distribution *c(S, f/f₀)* (lower contour plot) and the corresponding one-dimensional *c(S)* projection (upper trace). The frictional ratio (*f/f₀*) describes the deviation from an ideal spherical shape; lower *f/f₀* values indicate a more compact, globular protein, whereas higher values reflect an elongated or partially unfolded conformation. Sedimentation coefficients were corrected for water and 20 ºC ($S_{20,w}$). (A) Apo protein. (B) Protein + 550 μM Ca(II). (C) Protein + 2 mM Ca(II). (D) Protein + 550 μM Ca(II) + 27.5 μM Mn(II). All samples were analyzed in 75 mM HEPES (pH 7.5), 100 mM NaCl. Fitting parameters and derived results are reported in **Tables S11** and **S13**, respectively.

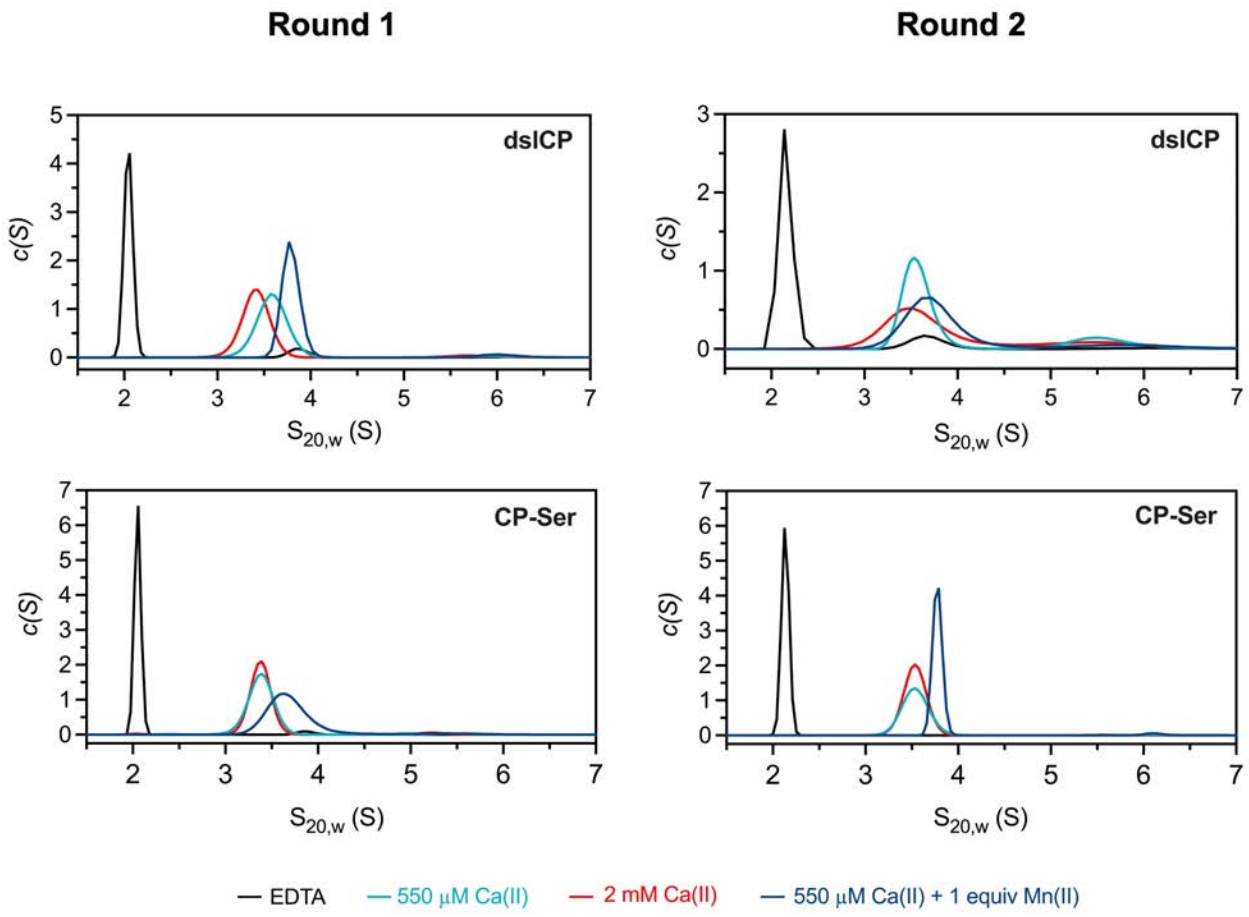

Figure S37. Un-normalized *c(S)* distributions from SV-AUC analysis of dsICP (*top*) and CP-Ser (*bottom*) from the two independent SV-AUC experiments (Round 1, *left*; Round 2, *right*). Samples (27.5 μM protein) were analyzed in the apo state or after incubation with 20 equiv Ca(II) (550 μM) ± 1 equiv Mn(II), or with physiological levels of Ca(II) (2 mM), as indicated. All samples were analyzed in 75 mM HEPES (pH 7.5), 100 mM NaCl. Sedimentation coefficients were corrected for water and 20 ºC ($S_{20,w}$). Fitting parameters and derived results are reported in **Tables S11** and **S12**, respectively.

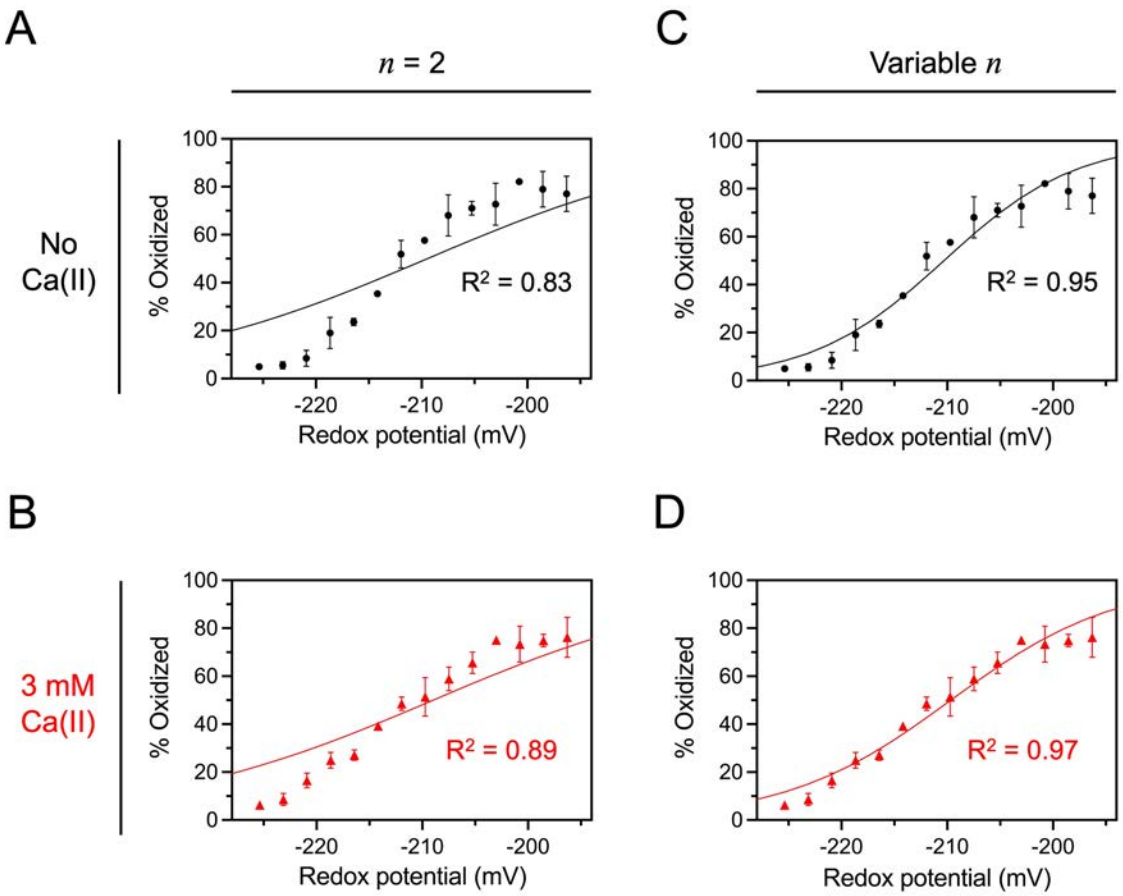

Figure S38. Nernst equation fits to dslCP midpoint potential data. (A) No-Ca(II) and (B) +Ca(II) E_m plots were fitted to a 2-electron reaction at 37 ºC (see Supplementary Discussion). Note how the Nernst equation approaches 0% oxidation for low (very negative) mV values and 100% for high mV values, contrary to the data points which plateau at ~80% oxidized protein. Furthermore, n = 2 results in a slope that is too shallow. The same fit was also performed assuming a variable n, for both (C) no-Ca(II) and (D) Ca(II)-replete E_m plots. The fits are better, although the asymptotes are not representative of the data.

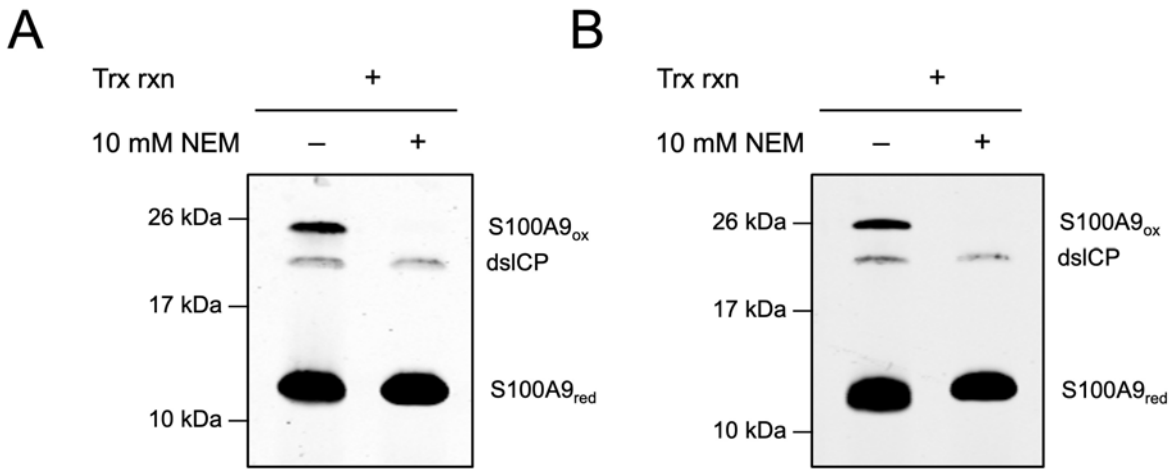

Figure S39. N-ethylmaleimide (NEM) is required to prevent adventitious A9 oxidation during SDS-PAGE sample storage and handling. (A) dslCP was incubated with Trx (2.5 μM), TrxR (0.05 μM) and NADPH (2.5 mM) for 1 h. Then, the reaction was treated with either DMSO (control), or 10 mM NEM. After 10 min, the samples were subjected to SDS-PAGE followed by α-A9 Western blotting. (B) The same samples as in part A were analyzed by α-A9 Western blotting after 48 h of storage at −20 ºC, revealing no A9 oxidation during that time following NEM treatment.

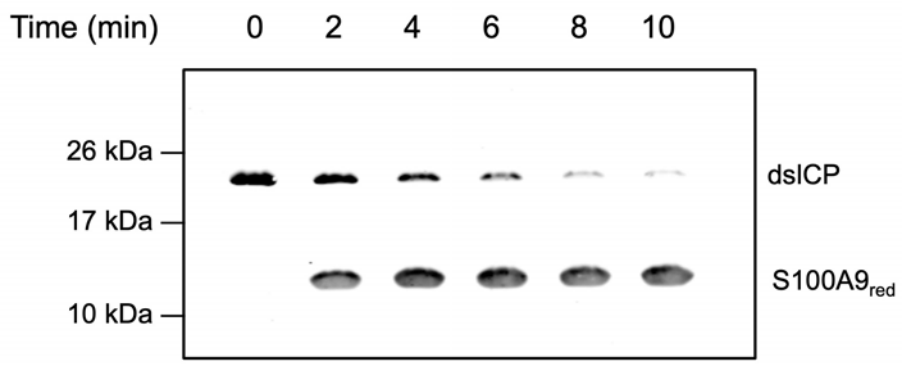

Figure S40. 0–10 min time course for dslCP reduction by the Trx system. dslCP was incubated with Trx (2.5 μM), TrxR (0.05 μM) and NADPH (2.5 mM), and samples were quenched with 10 mM NEM after the following times: 0 min, 2 min, 4 min, 6 min, 8 min and 10 min. Samples were subjected to SDS-PAGE and visualized by α-A9 Western blotting.

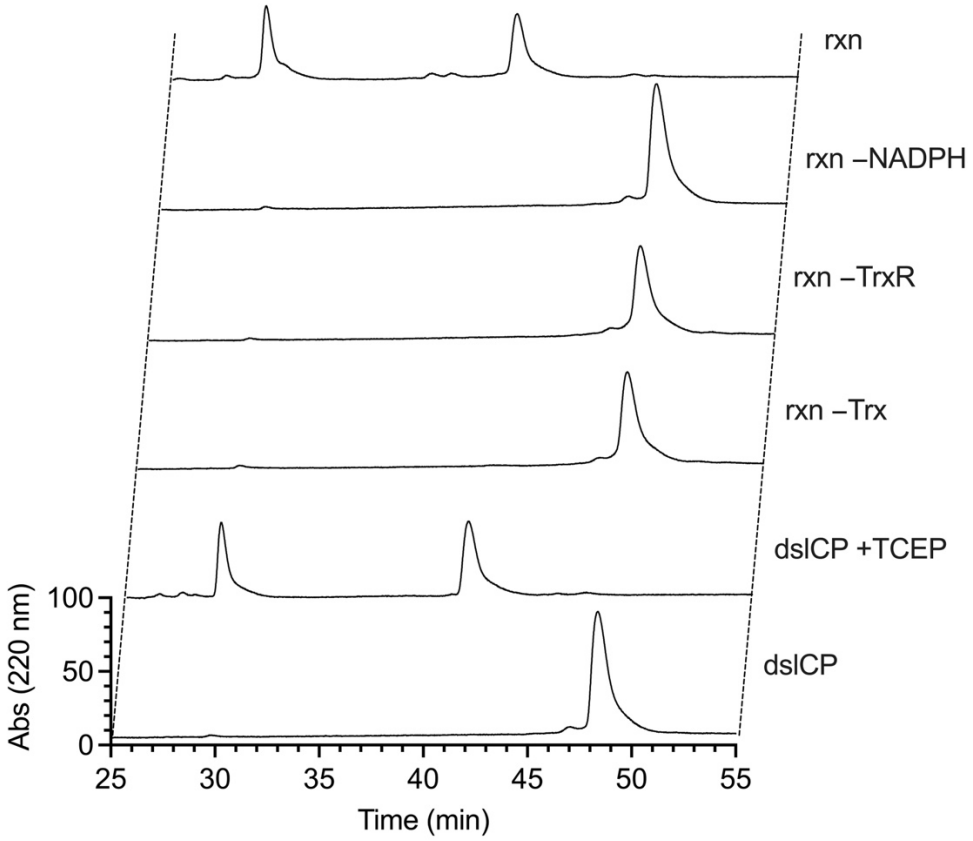

Figure S41. Thioredoxin reaction controls. dslCP was incubated with Trx (2.5 μM), TrxR (0.05 μM) and NADPH (2.5 mM) for 3 h ("rxn"); Trx, TrxR and NADPH were omitted one at a time as shown. dslCP was also treated with TCEP as a positive control for $S100A8_{red}$ and $S100A9_{red}$ peaks by HPLC.

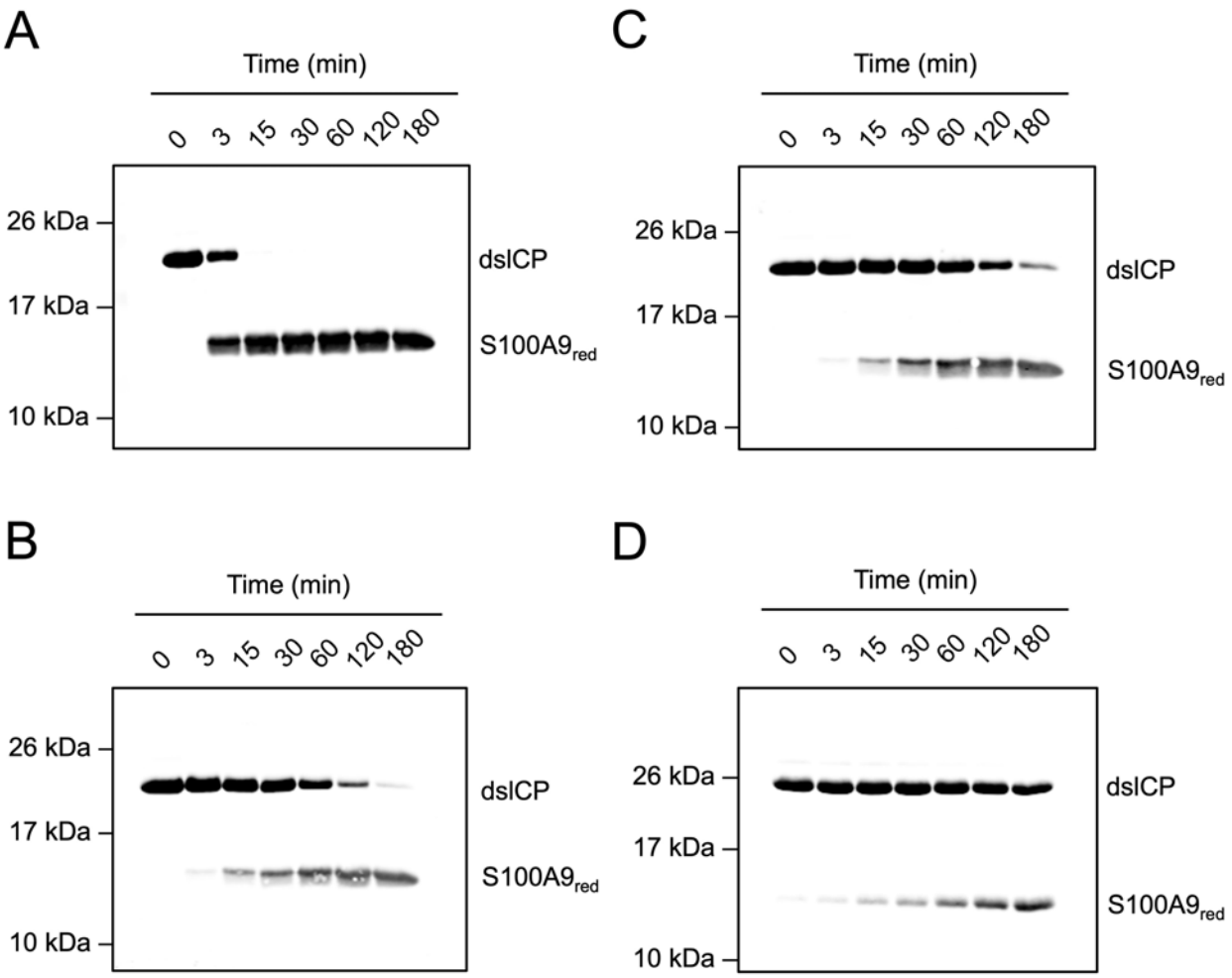

Figure S42. Uncut Western blots from **Figure 9B** of the main text. dslCP was incubated with Trx (2.5 μM), TrxR (0.05 μM) and NADPH (2.5 mM) and either: (A) no added Ca(II)/M(II); (B) 2 mM Ca(II); (C) 2 mM Ca(II) + 1 equiv Mn(II); or (D) 2 mM Ca(II) + 1.9 equiv Zn(II). Samples were taken at the indicated timepoints, subjected to SDS-PAGE, and visualized by α-A9 Western blotting.

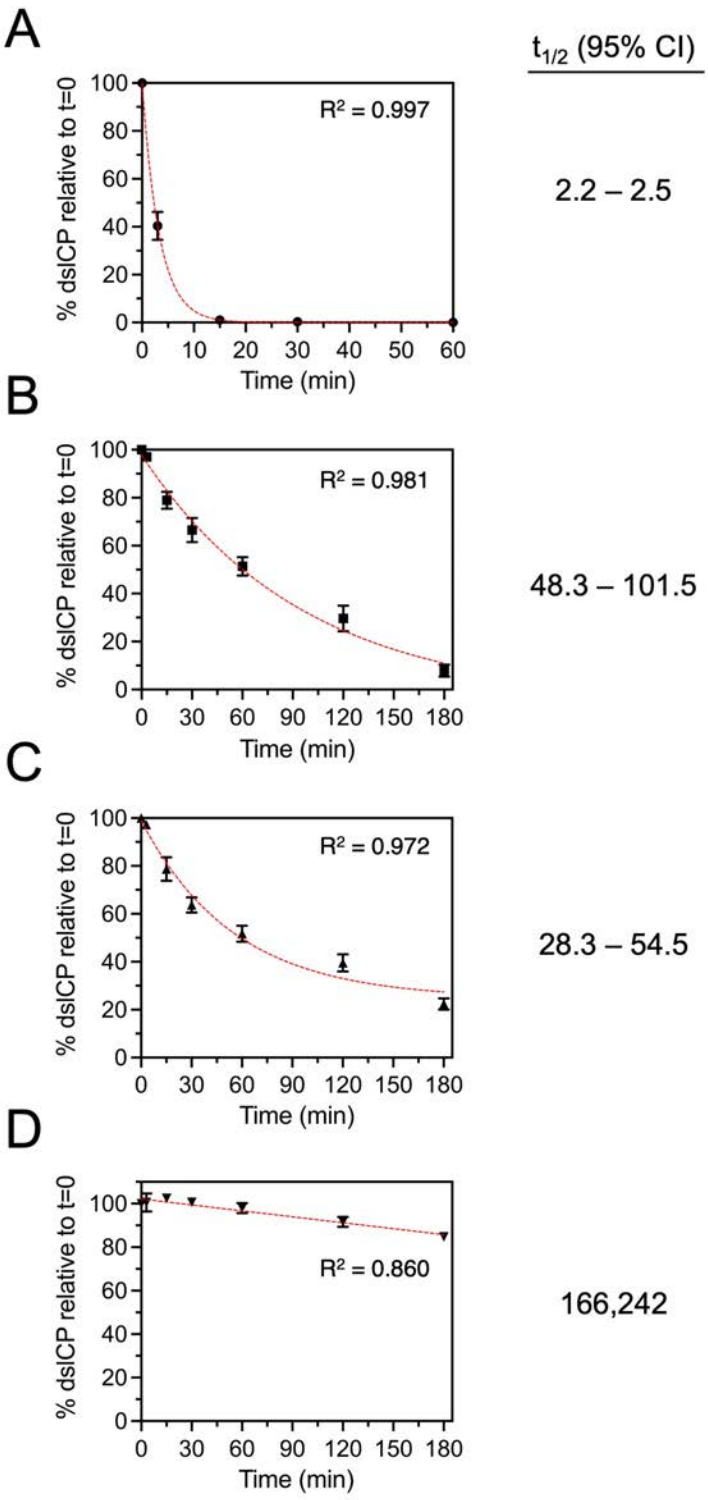

Figure S43. dsICP reduction data from **Figure 9C** in the main text (black dots) alongside exponential decay fits (dashed red lines) and associated $t_{1/2}$ 95% confidence intervals (CI; right). (A) No added Ca(II)/M(II) (B) 2 mM Ca(II) (C) 2 mM Ca(II) + 1 equiv Mn(II) (D) 2 mM Ca(II) + 1.9 equiv Zn(II). Note: for D, the fit could not give a precise CI, so the $t_{1/2}$ value is shown instead.

Supplementary Tables

Table S1. Sequences and molecular weights of S100A8 and S100A9. Cysteines C42(A8) and C3(A9) are highlighted in red and underlined.

Protein	Amino acid sequence	M.W. (kDa)
S100A8	MLTELEKALNSIIDVYHKYSLIKGNFHAVYRDDLKKLLETECP QYIRKKGADVWFKELDINTDGAVNFQEFLILVIKMGVAAHKK SHEESHKE	10.8
S100A9	MTCKMSQLERNIETIINTFHQYSVKLGHPDTLNQGEFKELVR KDLQNFLKKENKNEKVIEHIMEDLDTNADKQLSFEEFIMLMA RLTWASHEKMHEGDEGPGHHHKPGLGEGTP	13.2

Table S2. Identities and molecular weights of oxidized CP species.

Species abbreviation	Molecular identity	M.W. (kDa)
dslCP	C42(A8)-S-S-C3(A9)	24.0
$A9_{ox}$	C42(A8)-S-S-C42(A8')	26.4
$A8_{ox}$	C3(A9)-S-S-C3(A9')	21.6

Table S3. Metal ion stocks used.

Metal	Compound	Stated purity	Supplier
Ca	$CaCl_2 \cdot 2H_2O$	BioUltra, ≥ 99.5%	Sigma #21097
Mn	$MnCl_2 \cdot 4H_2O$	99.99% trace metal basis	Sigma #203734
Fe	$(NH_4)_2Fe(SO_4)_2 \cdot 6H_2O$	99.99% trace metal basis	Sigma #450278
Co	$CoCl_2 \cdot H_2O$	99.999% trace metal basis	Sigma #203084
Ni	$NiCl_2 \cdot 6H_2O$	99.999% trace metal basis	Sigma #203866
Cu	$CuSO_4 \cdot 5H_2O$	99.999% trace metal basis	Sigma #203165
Zn	$ZnSO_4 \cdot H_2O$	≥99.9% trace metal basis	Sigma #307491
Fe(III)	$FeCl_3$, anhydrous	≥99.99% trace metals basis	Sigma #451649

Table S4. Molecular weights and extinction coefficients of commercially purchased proteins.

Protein	Supplier / cat #	M.W. (kDa)	ε (M^{-1} cm^{-1}) *
Thioredoxin, human	Sigma #T8690	14	8,500
Thioredoxin reductase, from rat liver	Sigma #T9698	55	59,000
Trypsin	Affymetrix #22725	23.2	30,000
Human neutrophil elastase	Fisher Scientific #50-203-6611	28.5	19,500

* Extinction coefficients were calculated from the amino acid sequence using the ProtParam tool available on the ExPASy server.[S16]

Table S5. Theoretical vs. observed *m/z* of CP species (Q-TOF MS). O_n indicates dslCP variants with n × MetO residues.

Species	Theoretical *m/z*	Observed *m/z*	Δ (ppm)
$A8_{red}$	10,834.51	10,834.65	12.9
$A9_{red}$ −Met1	13,110.81	13,110.83	1.5
dslCP $-Met1_{A9}$	23,943.31	23,943.40	3.8
dslCP O_1 $-Met1_{A9}$	23,959.31	23,959.40	3.7
dslCP O_2 $-Met1_{A9}$	23,975.31	23,975.60	12.1
dslCP O_3 $-Met1_{A9}$	23,991.31	23,991.60	12.1
dslCP O_4 $-Met1_{A9}$	24,007.31	24,007.60	12.1
dslCP O_5 $-Met1_{A9}$	24,023.31	24,023.60	12.1
dslCP O_6 $-Met1_{A9}$	24,039.30	24,037.40	79.0

Table S6. Quantification of free thiols in CP and dslCP using DTDP assay. Data are mean ± SD (*n* = 3). These values indicate 2 and 0 free thiols for CP and dslCP, respectively.

Species	Free thiols (estimate)
CP	1.68 ± 0.02
dslCP	-0.07 ± 0.02

Table S7. Theoretical and observed *m/z* values for dslCP tryptic peptides detected in **Figures S7–S8**. The LLETECPQYIR–TCK peptide contains a disulfide bond between the cysteine residues of the two peptides.

Tryptic product (amino acid sequence)	Theoretical *m/z*	Observed *m/z*	Mass Error (ppm)
TCK	351.1697 (1+)	351.1710	+3.7
LLETECPQYIR	1364.6879 (1+)	1364.6890	+0.8
LLETECPQYIR–TCK	856.9210 (2+)	856.9245	+4.1

Table S8. Thermal denaturation melting temperatures for dslCP and CP in the absence and presence of 2 mM Ca(II). Literature values are indicated where available.

Protein	2 mM Ca(II)	Fit	T_m1 (ºC)	T_m2 (ºC)	Literature value (ºC)
dslCP	-	1-state Boltzmann (Equation 1)	73.9 ± 0.9	--	N/A
	-	2-state Boltzmann Equation (2)	75.3*	85.9*	N/A
	+	1-state Boltzmann (Equation 1)	85.2 ± 0.2	--	N/A
CP	-	1-state Boltzmann (Equation 1)	73.1 ± 0.1	--	59 (ref[S1])
	+	1-state Boltzmann (Equation 1)	85.6 ± 0.1	--	79 (ref[S1])

*Individual replicates that appeared to have a non-singular transition were combined and fitted to obtain these values. Errors could not be extracted from the fit. *n* = 7.

Table S9. Molecular weights from SEC chromatograms of dslCP and CP in the absence and presence of 2 mM Ca(II). See **Figure S12** for the standard curve used.

Protein	2 mM Ca(II)	Elution volume (mL)	M.W. of main peak (kDa)
dslCP	-	11.1	36
	+	10.5	49
CP	-	11.1	36
	+	10.4	47

Table S10. Strains used in this study.

Species	Strain	Source
Staphylococcus aureus	USA300 JE2	NARSA repository
Escherichia coli	CFT073 (ATCC 700928)	ATCC
Klebsiella pneumoniae	ATCC 13883	Walsh Lab
Salmonella enterica serovar Typhimurium	IR715	Raffatellu Lab
Acinetobacter baumannii	ATCC 17978	ATCC
Pseudomonas aeruginosa	UCBPP-PA14	Newman Lab
Candida albicans	SC5314 (ATCC MYA-2876)	Lindquist Lab

Table S11. Parameters used for SV-AUC *c(S)* analyses of dslCP and CP-Ser.

Parameter	Units	Buffer Composition†	Value
Solvent Density (ρ)*	g mL^{-1}	Buffer + 1.35 mM EDTA	1.0084
		Buffer + 550 μM $CaCl_2$	1.0082
		Buffer + 2 mM $CaCl_2$	1.0084
		Buffer + 550 μM $CaCl_2$ + 27.5 μM $MnCl_2$	1.0083
Solvent Viscosity (η)*	P	Buffer + 1.35 mM EDTA	0.01057
		Buffer + 550 μM $CaCl_2$	0.01056
		Buffer + 2 mM $CaCl_2$	0.01056
		Buffer + 550 μM $CaCl_2$ + 27.5 μM $MnCl_2$	0.01056
Partial Specific Volume ($\bar{\upsilon}$)*	mL g^{-1}	dslCP	0.738
		CP-Ser	0.738

† Buffer = 75 mM HEPES, 100 mM NaCl, pH 7.5
* Determined from chemical composition using SEDNTERP

Table S12. Parameters derived from SV-AUC *c(S)* analyses of dsICP and CP-Ser.

Species	**Replicate**	***c(S)* Analysis**						**Global f/f_0**
		Major Species			Minor Species			
		$S_{20,w}$	*% Signal*	M_w *(kDa)*	$S_{20,w}$	*% Signal*	M_w *(kDa)*	
dsICP + 1.35 mM EDTA	1	2.1	88.5	23.6	3.9	8.2	61.6	1.4
	2	2.1	82.8	24.0	3.6	12.5	53.7	1.3
dsICP + 550 μM Ca(II)	1	3.4	93.2	43.0	5.9	4.5	98.1	1.3
	2	3.5	68.1	54.7	5.5	20.0	108	1.4
dsICP + 2 mM Ca(II)	1	3.6	93.8	47.4	6.0	4.0	104	1.2
	2	3.5	60.1	46.2	5.5	16.7	90.3	1.2
dsICP + 550 μM Ca(II) + 1 equiv Mn(II)	1	3.8	91.6	49.0	6.0	5.2	98.1	1.2
	2	3.7	72.7	58.6	5.7	11.4	118	1.4
CP-Ser + 1.35 mM EDTA	1	2.1	95.8	22.9	3.8	3.4	57.9	1.4
	2	2.1	94.9	23.5	-	-	-	1.3
CP-Ser + 2 mM Ca(II)	1	3.4	96.3	44.4	5.4	2.6	87.1	1.3
	2	3.5	95.9	46.0	6.2	2.1	91.3	1.2
CP-Ser + 550 μM Ca(II)	1	3.4	91.7	45.2	2.0	0.8	93.1	1.3
	2	3.5	98.8	46.7	5.6	0.6	114	1.2
CP-Ser + 550 μM Ca(II) + 1 equiv Mn(II)	1	3.6	92.9	46.2	5.3	5.4	76.3	1.2
	2	3.8	97.6	47.2	6.1	2.4	97.1	1.2

All fits had RMSD ≤ 0.003.

Table S13. Parameters derived from SV-AUC *c(S,f/f₀)* analyses of dsICP and CP-Ser.

Species	Replicate	*c(S,f/f₀)* Analysis					
		Peak 1			Peak 2		
		$S_{20,w}$	M_w (kDa)	f/f_0	$S_{20,w}$	M_w (kDa)	f/f_0
dsICP + 1.35 mM EDTA	1	2.1	22.8	1.4	-	-	-
	2	2.1	23.2	1.3	3.5	33.3	1.0
dsICP + 550 μM Ca(II)	1	3.4	40.1	1.2	-	-	-
	2	3.5	45.5	1.3	5.3	97.2	1.4
dsICP + 2 mM Ca(II)	1	3.4	46.7	1.3	-	-	-
	2	3.4	40.3	1.3	5.5	66.4	1.2
dsICP + 550 μM Ca(II) + 1 equiv Mn(II)	1	3.6	42.7	1.2	-	-	-
	2	3.6	47.5	1.3	5.6	99.1	1.4
CP-Ser + 1.35 mM EDTA	1	2.0	23.2	1.4	-	-	-
	2	2.0	20.6	1.3	-	-	-
CP-Ser + 550 μM Ca(II)	1	3.4	39.3	1.2	-	-	-
	2	3.4	38.2	1.2	-	-	-
CP-Ser + 2 mM Ca(II)	1	3.4	47.4	1.4	-	-	-
	2	3.3	37.2	1.2	-	-	-
CP-Ser + 550 μM Ca(II) + 1 equiv Mn(II)	1	3.6	44.0	1.3	-	-	-
	2	3.6	41.1	1.2	-	-	-

All fits had RMSD ≤ 0.003.

Table S14. Nernst equation fitting results of −Ca(II) E_m data.

Model	Equation	E_m	*n*	*h*	Y_{min}	Y_{max}	R^2
Nernst (*n* = 2)	(7)	−209.5 ± 2.4	-	-	-	-	0.83
Nernst (variable *n*)	(8)	−210.3 ± 0.8	4.3	-	-	-	0.95
4P Hill-Nernst	(9)	−213.5 ± 0.9	-	3.7	1.2	79.6	0.97

Table S15. Nernst equation fitting results of +Ca(II) E_m data.

Model	Equation	E_m	*n*	*h*	Y_{min}	Y_{max}	R^2
Nernst (*n* = 2)	(7)	−209.0 ± 1.7	-	-	-	-	0.89
Nernst (variable *n*)	(8)	−209.7 ± 0.7	3.4	-	-	-	0.97
4P Hill-Nernst	(9)	−213.3 ± 2.4	-	2.3	0	81.1	0.96

Table S16. Midpoint potential values of a variety of important redox-active biomolecules, and a selection of prokaryotic and eukaryotic cysteine-containing proteins.

Species	Source	Description	E_m (mV)	Ref.
Bovine pancreatic trypsin inhibitor (aprotinin)	*Bos taurus*	Potent serine protease inhibitor	−470*	S17
Metallothionein	Mammalian	Zinc-binding, redox signaling	< −366	S18
ResA	*B. subtilis*	Cytochrome c maturation	−345	S19
DTT_{ox}/DTT_{red}	-	Small molecule reducing agent	−330	S20
$NADP^+/NADPH^{\S}$	-	Nicotinamide electron and hydride donor	−320	S21
βII-Tryptase (C220–C248 only)	*H. sapiens*	Mast cell serine protease	−301	S22
S. cerevisiae Trx1	*S. cerevisiae*	Major yeast cytosolic redox protein	−275 ± 1	S23
E. coli Trx1	*E. coli*	Primary prokaryotic cytosolic redox protein	−270	S24
S. cerevisiae Trx2	*S. cerevisiae*	Mitochondrial/cytosolic antioxidant	−265 ± 10	S23
NrdH-redoxin	*E. coli*	Electron donor for ribonucleotide reductase	−249	S25
GSH/GSSG	-	Abundant low-molecular-weight cellular redox buffer	−245	S26
E. coli Grx1	*E. coli*	Cytosolic redox enzyme	−233	S27
Human Glutaredoxin 1 (hGrx1)	*H. sapiens*	GSH-dependent cytosolic reductant	−232	S28
Human Thioredoxin 1	*H. sapiens*	Primary human cytosolic redox regulator	−230	S29
Human Glutaredoxin 2 (hGrx2)	*H. sapiens*	GSH-dependent cytosolic reductant	−221	S28
Coenzyme A	-	Metabolic enzyme cofactor	−199 ± 2	S30
E. coli Grx3	*E. coli*	Cytosolic redox enzyme	−198	S27
Cysteine	-	Free amino acid	−188 ± 1	S30
TG2 (C370–C371)	*H. sapiens*	GTP-binding protein and transglutaminase	−184	S31
Protein disulfide isomerase (PDI)	*H. sapiens*	ER oxidative folding and isomerization	−175	S32
ERp57	*H. sapiens*	ER folding of heavily glycosylated proteins	−158	S33
DsbC	*E. coli*	Periplasmic disulfide bond isomerase	−130	S34
DsbG	*E. coli*	Periplasmic isomerase/repair	−125	S35
DsbA	*E. coli*	Primary periplasmic disulfide bond oxidase	−120	S36

*The exceptional stability of the disulfide bond in aprotinin is a consequence of tight packing and the hydrophobicity of the protein, which results in a high entropic penalty for the unfolded state.[S37]
[§]Refers to a nicotinamide adenine dinucleotide couple; all other values represent thiol-disulfide redox couples.

Supplementary References

S1 M. B. Brophy, J. A. Hayden and E. M. Nolan, *J. Am. Chem. Soc.*, 2012, **134**, 18089–18100.
S2 J. R. Stephan and E. M. Nolan, *Chem. Sci.*, 2016, **7**, 1962–1975.
S3 T. G. Nakashige, E. M. Zygiel, C. L. Drennan and E. M. Nolan, *J. Am. Chem. Soc.*, 2017, **139**, 8828–8836.
S4 T. G. Nakashige, J. R. Stephan, L. S. Cunden, M. B. Brophy, A. J. Wommack, B. C. Keegan, J. M. Shearer and E. M. Nolan, *J. Am. Chem. Soc.*, 2016, **138**, 12243–12251.
S5 Y. A. Wanniarachchi, P. Kaczmarek, A. Wan and E. M. Nolan, *Biochemistry*, 2011, **50**, 8005–8017.
S6 T. G. Nakashige, B. Zhang, C. Krebs and E. M. Nolan, *Nat. Chem. Biol.*, 2015, **11**, 765–771.
S7 E. M. Zygiel, A. O. Obisesan, C. E. Nelson, A. G. Oglesby and E. M. Nolan, *J. Biol. Chem.*, 2021, **296**, 100160.
S8 B. Schwyn and J. B. Neilands, *Anal. Biochem.*, 1987, **160**, 47–56.
S9 D. B. Alexander and D. A. Zuberer, *Biol. Fertil. Soils*, 1991, **12**, 39–45.
S10 J. R. Stephan, F. Yu, R. M. Costello, B. S. Bleier and E. M. Nolan, *J. Am. Chem. Soc.*, 2018, **140**, 17444–17455.
S11 L. S. Cunden, M. B. Brophy, G. E. Rodriguez, H. A. Flaxman and E. M. Nolan, *Biochemistry*, 2017, **56**, 5726–5738.
S12 Y. Zhang, F. B. L. Cougnon, Y. A. Wanniarachchi, J. A. Hayden and E. M. Nolan, *ACS Chem. Biol.*, 2013, **8**, 1907–1911.
S13 W. Maret, C. Jacob, B. L. Vallee and E. H. Fischer, *Proc. Natl. Acad. Sci. U. S. A.*, 1999, **96**, 1936–1940.
S14 A. P. Lothrop, G. W. Snider, E. L. Ruggles, A. S. Patel, W. J. Lees and R. J. Hondal, *Biochemistry*, 2014, **53**, 654–663.
S15 J. Chaudière, *Int. J. Mol. Sci.*, 2023, **24**, 10109.
S16 E. Gasteiger, C. Hoogland, A. Gattiker, S. Duvaud, M. R. Wilkins, R. D. Appel and A. Bairoch, in *The Proteomics Protocols Handbook*, ed. J. M. Walker, Humana Press, Totowa, NJ, 2005, pp. 571–607.
S17 D. P. Goldenberg, L. S. Bekeart, D. A. Laheru and J. D. Zhou, *Biochemistry*, 1993, **32**, 2835–2844.
S18 W. Maret and B. L. Vallee, *Proc. Natl. Acad. Sci. U. S. A.*, 1998, **95**, 3478–3482.
S19 C. L. Colbert, Q. Wu, P. J. A. Erbel, K. H. Gardner and J. Deisenhofer, *Proc. Natl. Acad. Sci. U. S. A.*, 2006, **103**, 4410–4415.
S20 W. W. Cleland, *Biochemistry*, 1964, **3**, 480–482.
S21 V. Cracan, D. V. Titov, H. Shen, Z. Grabarek and V. K. Mootha, *Nat. Chem. Biol.*, 2017, **13**, 1088–1095.
S22 K. M. Cook, H. P. McNeil and P. J. Hogg, *J. Biol. Chem.*, 2013, **288**, 34920–34929.
S23 J. T. Mason, S.-K. Kim, D. B. Knaff and M. J. Wood, *Biochemistry*, 2006, **45**, 13409–13417.
S24 G. Krause, J. Lundström, J. L. Barea, C. Pueyo de la Cuesta and A. Holmgren, *J. Biol. Chem.*, 1991, **266**, 9494–9500.
S25 A. Jordan, F. Åslund, E. Pontis, P. Reichard and A. Holmgren, *J. Biol. Chem.*, 1997, **272**, 18044–18050.
S26 Z. Salamon, F. K. Gleason and G. Tollin, *Arch. Biochem. Biophys.*, 1992, **299**, 193–198.
S27 F. Åslund, K. D. Berndt and A. Holmgren, *J. Biol. Chem.*, 1997, **272**, 30780–30786.
S28 J. Sagemark, PhD thesis, Karolinska Institutet, Stockholm, 2008.

S29 W. H. Watson, J. Pohl, W. R. Montfort, O. Stuchlik, M. S. Reed, G. Powis and D. P. Jones, *J. Biol. Chem.*, 2003, **278**, 33408–33415.
S30 D. A. Keire, E. Strauss, W. Guo, B. Noszal and D. L. Rabenstein, *J. Org. Chem.*, 1992, **57**, 123–127.
S31 X. Jin, J. Stamnaes, C. Klöck, T. R. DiRaimondo, L. M. Sollid and C. Khosla, *J. Biol. Chem.*, 2011, **286**, 37866–37873.
S32 J. E. Chambers, T. J. Tavender, O. B. V. Oka, S. Warwood, D. Knight and N. J. Bulleid, *J. Biol. Chem.*, 2010, **285**, 29200–29207.
S33 E.-M. Frickel, P. Frei, M. Bouvier, W. F. Stafford, A. Helenius, R. Glockshuber and L. Ellgaard, *J. Biol. Chem.*, 2004, **279**, 18277–18287.
S34 A. Zapun, D. Missiakas, S. Raina and T. E. Creighton, *Biochemistry*, 1995, **34**, 5075–5089.
S35 M. van Straaten, D. Missiakas, S. Raina and N. J. Darby, *FEBS Lett.*, 1998, **428**, 255–258.
S36 A. Zapun, J. C. A. Bardwell and T. E. Creighton, *Biochemistry*, 1993, **32**, 5083–5092.
S37 T. E. Creighton and D. P. Goldenberg, *J. Mol. Biol.*, 1984, **179**, 497–526.